Universidade do Minho
Escola de Engenharia

Ana Isabel Machado da Silva

Engineering of specific bacteriophages for early diagnosis of Alzheimer's disease

Outubro de 2016

Engineering of specific bacteriophages for early diagnosis of Alzheimer's disease
Ana Isabel Machado da Silva
Uminho | 2016

Universidade do Minho
Escola de Engenharia

Ana Isabel Machado da Silva

Engineering of specific bacteriophages for early diagnosis of Alzheimer's disease

Dissertação de Mestrado
Mestrado em Bioengenharia

Trabalho efetuado sob a orientação da
Doutora Ivone Marisa Pereira Martins
e do **Doutor Leonardus Dorothea Kluskens**

Outubro de 2016

ACKNOWLEDGMENTS

Utilizo este pequeno espaço para tentar de alguma maneira agradecer a todos que direta ou indiretamente ajudaram a tornar esta dissertação possível.

Á minha orientadora, Ivone Martins, agradeço a disponibilidade, orientação e todo o apoio prestado ao longo deste trabalho.

Ao meu co-orientador, professor Leon Kluskens, agradeço (em memória) a sua simpatia e por sempre se ter mostrado disponível para me ajudar.

I would also like to thank to Helmut Kessels and Neils Reinders for providing essential material for the achievement of this work. Adicionalmente, pelo auxílio na análise na microscopia, obrigada à Diana Vilas Boas do CEB e ao João Cruz Sousa do ICVS.

Débora, obrigada! Obrigada pelo apoio incondicional, pela ajuda constante, por tudo que me fizeste aprender quando não tinhas obrigação nenhuma de o fazer. Agradeço mesmo, pois sem ti tudo teria sido muito mais difícil (tenho a noção de quanto te chateei).

Um especial obrigada às meninas da PBMS: Adriana, Carla, Diana, Joana, Márcia e Ritinha, e também ao único homem entre as mulheres, Rodrigo. Foi um prazer poder ter a oportunidade de partilhar o espaço de trabalho convosco e sem vós estes meses teriam sido muito menos felizes. À Ângela, ao Daniel e ao Ricardo, mesmo não pertencendo à PBMS, agradeço também por terem feito parte deste ano e terem estado cá quando precisava. Às meninas das portas do lado, Bioprocessos e LBA, obrigada por toda a ajuda sempre que precisei, e eu sei que precisei muito.

Ao Ricardo Fernandes, obrigada me teres acompanhado nestes últimos anos. Agradeço também o carinho, apoio e por saberes lidar comigo mesmo nos meus piores dias.

Agradeço também à minha família e aos meus amigos que mesmo não estando aqui referenciados me apoiaram durante este último ano.

Ao meu irmão, agradeço as palavras de apoio, os exemplos que me foste dando e os conselhos do que fazer e não fazer. Obrigada pelos momentos de desanuvio e também por ouvires até quando o tema não te dizia nada.

Por último, sabendo que este será o agradecimento mais importante, obrigada pai e mãe! Obrigada por tudo o que fizeram por mim, obrigada pela educação, por me darem sempre o melhor, mesmo quando isso significava fazerem os sacrifícios que fizeram. Espero agora poder retribuir tudo o que me deram e um dia ser metade da pessoa que vocês são. A vós dedico este trabalho!

ABSTRACT

Alzheimer's disease (AD) is a neurodegenerative disorder and the most common form of dementia. It affects mostly people over 65 years and the main symptoms are loss of memory and cognitive functions. Biologically, it is thought that this disease is characterized by the accumulation of a small peptide called amyloid beta (Aβ). This peptide aggregates into oligomers, the presumed real reason of synaptic disruption and memory loss. Recently, two sequences were described to recognize Aβ oligomers, the Aβ 30-39 (AIIGLMVGGV) and Aβ 33-42 (LMVGGVVIA).

So far no accurate diagnosis exists increasing the need to develop tools for early diagnosis. Nevertheless, it is difficult to access the brain due to the presence of the blood brain barrier (BBB). Based on the ability of the bacteriophage M13 to cross the BBB and the existence of sequences that recognize the Aβ, the main goal of this work was to develop an early diagnosis tool for AD diagnosis through the engineering of the bacteriophage M13 in order to express the Aβ sequences on its capsid. Different approaches were used to genetically manipulate the M13 genome in order to clone the AB sequences, and it was possible to insert only the last four amino acids of the Aβ 30-39 sequence (VGGV). With this modified phage particle, immunohistochemistry assays were performed using AD model tissue from the hippocampus of a double transgenic mice APPswe/PS1dE9. The results of these assays proved promising, with a significant affinity of the modified phage towards the AD model tissue, and possibly to the Aβ oligomers.

In short, the overall objectives of this work were accomplished, leaving the opportunity for further work to improve and validate this phage particle as an AD diagnosis tool.

RESUMO

A Doença de Alzheimer (DA) é uma doença neurodegenerativa e a forma mais comum de demência. Esta doença afeta maioritariamente pessoas com mais de 65 anos e os seus sintomas são a perda gradual de memória e de funções cognitivas. Biologicamente, pensa-se que a principal causa desta doença é a acumulação de um pequeno péptido chamado amiloide-beta (Aβ) na sua forma oligomérica. Recentemente foram descritas duas sequências que mostraram uma elevada afinidade aos oligómeros de Aβ, especificamente as sequências Aβ 30-39 (AIIGLMVGGV) e Aβ 33-42 (LMVGGVVIA).

Até ao momento não foi descoberto nenhuma ferramenta de diagnóstico para DA. Um dos motivos principais para a falta de diagnóstico é a existência da barreira hematoencefálica. Esta barreira impede o acesso de moléculas, vírus entre outros ao sistema nervoso central. Tendo em conta os estudos que demonstram a capacidade do bacteriófago M13 para ultrapassar a barreira hematoencefálica e também a existência de sequências capazes de reconhecer Aβ na sua forma oligomérica, o objetivo principal deste trabalho foi a criação de uma plataforma de diagnóstico precoce para DA através da modificação genética do fago M13 de modo a este expressar à sua superfície as sequências Aβ. Durante a elaboração deste trabalho diferentes metodologias foram realizadas na tentativa de modificar geneticamente o fago M13. Através destas abordagens foi possível a obtenção de uma partícula fágica modificada possuindo na sua superfície os últimos quatro aminoácidos da sequência Aβ 30-39 (VGGV). Ensaios de imunohistoquímica foram realizados de modo a avaliar a afinidade do fago modificado para o tecido do hipocampo de ratos modelo da DA. Os resultados obtidos nestes ensaios mostraram-se promissores, sugerindo que o novo fago possui elevada afinidade para os oligómeros Aβ.

Resumidamente, pode dizer-se que os objetivos gerais deste trabalho foram alcançados, deixando oportunidade de trabalhos futuros para o desenvolvimento de um modelo de diagnóstico para a DA, utilizando a partícula fágica obtida.

INDEX

LIST OF FIGURES

LIST OF TABLES

LIST OF ABBREVIATIONS

AD: Alzheimer's Disease

APP: Amyloid Precursor Protein

Aβ: Amyloid-β

BBB: Blood Brain Barrier

BSA: Bovine Serum Albumin

$CaCl_2$: Calcium Chloride

CDR: Complementarity Determining Regions

CED: Convection Enhanced Delivery

ChEIs: Cholinesterase Inhibitors

CNS: Central Nervous System

CSF: Cerebrospinal Fluid

CT: Computed Tomography

DMSO: Dimethylsulfoxide

DNA: Deoxyribonucleic Acid

DOX: Doxorubicin

dsDNA: Double Strand DNA

EDTA: Ethylenediamine Tetraacetic Acid

FDA: Food and Drug Administration

fMRI: functional Magnetic Resonance Imaging

IHC: Immunohistochemistry

IPTG: Isopropyl β-D-1-thiogalactopyranoside

KCl: Potassium Chloride

LB: Lysogeny Broth

MCI: Mild Cognitive Impairment

$MgCl_2$: Magnesium Chloride

MMSE: Mini-Mental State Examination

MRI: Magnetic Resonance Imaging

NaCl: Sodium Chloride

NHS: N-Hydroxysuccinimide

NMDA: N-methyl-D-aspartate

OD: Optical Density

PBS: Phosphate Buffered Saline

PCR: Polymerase Chain Reaction

PEG: Polyethylene Glycol

PES: Polyethersulfone

PET: Positron Emission Tomography

PFU: Plate Forming Unit

rpm: Rotations Per Minute

SBP: Streptavidin Binding Peptide

SDS: Sodium Dodecyl Sulfate

SE: Succinimidyl Ester

SM: Saline Magnesium

SOC: Super Optimal Broth with Catabolite Repression

SPECT: Single Photon Emission Computed Tomography

ssDNA: Single Strand DNA

TAE: Tris Acetate EDTA

TBS: Tris-buffered Saline

TBST: TBS-Tween 20

TE: Tris-EDTA

TFP: Tetrafluorophenyl

X-Gal: 5-bromo-4-chloro-3-indolyl-β-D-galactoside

1. INTRODUCTION

1.1 Alzheimer's disease

In 1901, a patient known as Auguste Deter, was admitted to the Frankfurt hospital with memory and behavior problems. She was showing progressive cognitive impairment, focal symptoms, hallucinations, delusions, and psychosocial incompetence. Auguste Deter was studied for five years by Alois Alzheimer, a German physician, before her death in 1906 at the age of 57. Alzheimer's disease (AD) was described for the first time in 1907. When Alois Alzheimer examined the brain of Auguste under the microscope, he discovered that many brain cells had disappeared and had been replaced by tangles and plaques. After his observations Alzheimer described that Auguste was suffering from a form of dementia (Alzheimer, 1907). Although Alzheimer was first to describe it, the disease was only named after him in 1910 by Emil Kraepelin, a doctor who worked with Alzheimer (Lim & Lim, 2013; Maurer et al., 1997).

It is now known that AD is a neurodegenerative disease and the most common form of dementia. Because of this, the word "dementia" is sometimes used interchangeably with AD. However, there are other types of dementia such as vascular, Lewy body among others. Therefore it is important to know that dementia refers to a group of brain disorders, not only to AD. The single greatest risk factor for AD is age. It mainly affects people over the age of 65 but it may be manifested well before. According to the 2016 World Alzheimer Report, there are around 47 million people worldwide with AD and for 2050 the estimations are of 131 million people affected (Prince et al., 2016).

As people age, the brain undergoes a number of changes, in case of AD the brain slowly shrivels and dies. Nerve cells in the brain stop working and brain signals, that are essential for life, do not function properly. The major cell loss appears to be in the basal forebrain more specifically in the hippocampus, one of the most important brain structures involved in memory and learning. The communication between nerve cells is performed by synapses - a structure that allows a nerve cell to pass an electrical or chemical signal to another nerve cell. For this reason synapses are essential to a correct neuronal function. In AD a peptide called amyloid-β (Aβ) accumulates in the synapses, avoiding the signals and the essentials nutrients for cell life to be transmitted. Eventually the neurons die resulting in the loss of brain tissue. This series of

events leads to the loss of memory, mental and physical abilities severe enough to affect daily life (Carol Turkington, 2010; Sheng et al., 2015).

Although symptoms are observed only at an advanced age it is known that AD markers are present in the brain well before this stage (Lesné et al., 2013) . The progression of the disease can be categorized in three different stages. The first stage is known as Preclinical AD - the concentration changes of biomarkers such as the Aβ peptide may indicate the very earliest signs of the disease, before outward symptoms are visible. Currently, there are no clinical diagnostic criteria for this stage. The next stage is known as Mild Cognitive Impairment (MCI) and corresponds to a variety of symptoms, most commonly memory loss which does not significantly alter daily life. The last stage, Dementia due to AD is characterized by memory, thinking and behavioral symptoms that impair a person's ability to function in daily life (McKhann et al., 2011). The following Table demonstrates some of the criteria used to identify the stages of AD.

Table 1 Criteria to identify the different stages of AD *(Jack et al., 2011).*

Preclinical AD	Measurement of changes in biomarkers (such as brain imaging and spinal fluid chemistry), that indicate the very earliest signs of the disease, before outward symptoms are visible.
Mild cognitive Impairment due to AD	Mild changes in memory and thinking abilities, enough to be noticed and measured, but not impairment that compromises everyday activities and functioning.
Dementia due to AD	Memory, thinking and behavioral symptoms that impair a person's ability to function in daily life.

The course and duration of AD varies from person to person depending on multiple factors, including the age of the diagnosis and other medical issues. The later the disease is diagnosed the less lifetime is assigned to the patient. Even symptoms are expressed in different ways, some patients become very adept at hiding memory problems early on. For example, they will describe an object if they have trouble recalling its name or keep lists and calendars to help remember dates and events. Some people deny the fact that they forgot a few things for fear of

the disease, until noticing that they are not able to perform basic tasks, such as remember the way home or grandchildren names (Caselli & Reiman, 2013; Donoso, 2003).

1.1.1 AD Symptoms

As stated above the main symptom of AD is dementia. Symptoms of dementia usually include the gradual loss of memory and communication skills as well as a decline in the ability to think and reason clearly. The term dementia is used if the symptoms are severe enough to have an effect on a person's ability to carry out ordinary daily activities. Among the symptoms that usually characterize AD none is specific to a single stage of the disease (Dauwels et al., 2010).

As cognitive abilities continue to decline as the stage progresses, the person remembers less and less about current and recent events and may show some memory loss for personal history. As the age advances symptoms will become more intense and frequent. The patients begin to demonstrate difficulties in developing the reasoning. These difficulties are more noticed in actions like dealing with the house accounts or organize important documents. Personality alterations become more relevant where the patient begins to feel irritable, nervous and slightly aggressive. By this stage, patients can no longer be without help. Many patients became unable to remember major aspects of their lives, such as their address or telephone number, the names of close family members or where they went to college. Eventually, they may wander, be unable to engage conversation, seem inattentive and erratic in mood, appear uncooperative, lose bladder and bowel control and, in some cases become completely dependent on others for care, not even be able to feed themselves (Bäckman et al., 2004; Meek et al., 1998).

1.1.2 AD Causes

AD is characterized mainly by the presence of two markers: extracellular amyloid plaques and intracellular neurofibrillary tangles. The major constituent of the amyloid plaques is a 40-42 amino acid peptide termed amyloid-β (Aβ) (DeMattos et al., 2012).

The source of Aβ is the amyloid precursor protein (APP) that encodes an ubiquitous transmembrane protein, which has been postulated to play a role in cell movement and cell

adhesion (LaFerla et al., 2007). Degradation of APP arises via two pathways: the non-amyloidogenic and the amyloidogenic (or disease pathway) (Figure 1).

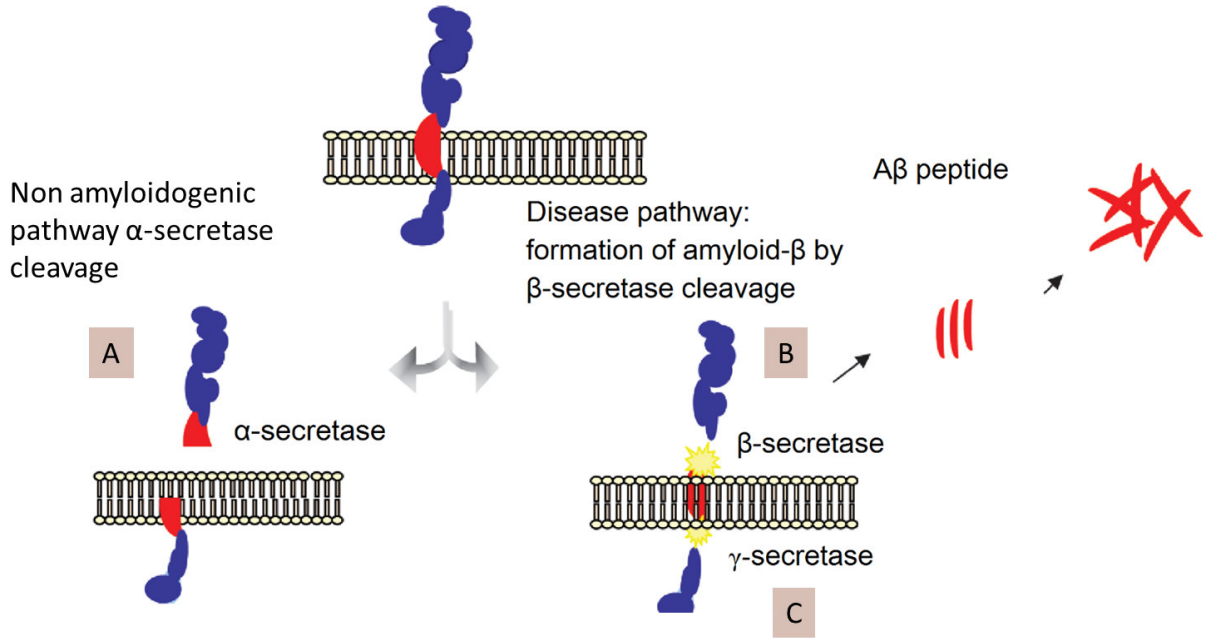

Figure 1 APP degradation. *Amyloidogenic and non-amyloidogenic pathways (Paula & Guimarães, 2009).*

In the non-amyloidogenic pathway, APP is cleaved by α -secretase (Figure 1A) within the Aβ domain off the APP protein preventing Aβ formation. In the disease pathway, the one that leads to AD, APP is cleaved by the enzyme β -secretase (Figure 1B), resulting in an intermediate of Aβ. This segment is then further processed by the complex ɣ -secretase (Figure 1C) and the product of this reaction is the Aβ peptide. Depending on where the ɣ -secretase cleaves the Aβ intermediate, previously cleaved by β -secretase, two types of Aβ molecule can be formed: one that contains 40 amino acids and other with 42 amino acids (Schu et al, 2012). The difference between these two monomers is the presence or absence of two residues on C-terminal (Ile^{41} and Ala^{42}). Despite this small difference, on a biological level the effect is quite notorious, Aβ 42 is deposited first during the development of AD and is more neurotoxic than Aβ 40 (Iwatsubo et al., 1994). The accumulation of these Aβ monomers will result in the formation of oligomers.

Although it is known that the principal component of amyloid plaques are Aβ fibrils (oligomers accumulation), studies suggest that the real cause of the synaptic disruption and memory loss is the Aβ in its oligomeric form. Aβ fibrils may contribute to worsening the disease but are thought to be the end product of Aβ self-association process rather than the predominant

pathogenic form (Frenkel et al., 2000; Haass & Selkoe, 2007). Despite the existence of different types of oligomers, all have been proved to be neurotoxic. In the brain and in the cerebrospinal fluid (CSF) of patients with AD, high concentrations of Aβ oligomers can be found, relative to healthy individuals. Some animal studies show that there is a decrease in the ability to retain memories and learning even before the formation of amyloid plaques, and that a higher concentration of oligomers is related to a more pronounced decline of cognitive functions (Shanmugam et al., 2008).

Oxidative stress, cellular damage and the presence of a high concentration of Aβ are all capable of activating both innate and humoral inflammatory process. Amyloid plaques are indeed co-localized with a broad variety of inflammation-related proteins and clusters of activated microglia and reactive astrocytes. Also, the loss of neuronal interconnections (synapses), is associated with decreased concentration of neurotransmitters, the chemical signals that are exchanged between neurons. One such neurotransmitter is acetylcholine, the decline of which is hypothesized to be one of the factors responsible for the intellectual deterioration observed in both normal ageing and in AD. These two major factors, the onset of the inflammatory response by toxic proteins and the synapses loss, lead to inflammation of the brain and consequent deterioration (Eikelenboom et al., 2010; Schmidt et al., 2002; Tiraboschi et al., 2004).

1.1.3 AD Diagnosis

A definitive diagnosis for AD is still inexistent, and the disease can only be confirmed *post-mortem* by autopsy (Brewer, 2012). However, there are some methods that allow an indirect diagnosis of the disease based on some criteria. The two main criteria for AD diagnosis are: (i) to identify the three stages of the disease, before symptoms such as memory loss occur and before one's ability to carry out everyday activities are affected; the original criteria require memory loss and a decline in thinking abilities severe enough to affect daily life and (ii) to incorporate biomarker tests able to measure biological changes in the brain associated with AD. These biomarkers are divided into two categories: biomarkers of Aβ accumulation, which are found in lower levels in the CSF, and biomarkers of neuronal degeneration or injury which measure the atrophy on the brain (Jack et al., 2011).

When a patient begin to show some of the characteristic symptoms of AD and the result of some of the criteria above is positive, there is a set of tests and techniques that allow indirect diagnosis (Nowotny et al., 2001).

a. *Diagnostic screens and tests*

The tests conducted for AD evaluation can go from the most basic, such as memory tests on paper, to the most complex tests in the brain. Usually the first step in diagnosis is to evaluate the memory capacity of the patient. For this, some questions are held to the individual and his family along with some quick memory tests.

The Folstein Mini-Mental State Examination (MMSE) is the most commonly used test to assess serial cognitive changes in AD. This consists of a 30-point questionnaire examining registration, attention and calculation, recall, language, ability to follow simple commands and orientation. While this test is a good indicator for the onset of the disease there are some flaws regarding its sensitivity, especially when the disease needs to be evaluated in a mild state. Even a perfect MMSE score does not exclude MCI or mild AD. Moreover, age and education affect performance on the MMSE (Dufouil et al., 2000).

The Clock Drawing Test is a rapid test for office-based practice. Although there is some disagreement about its use, it continues to provide information that facilitates diagnosis. Scores are based on the ability to draw the face of a clock with the hands pointing to the appropriate numbers of a designated time.

The 7-Minute Screen this test was developed for use at a memory disorders clinic. This test is a compilation of the temporal orientation test, enhanced cued recall, clock drawing, and verbal fluency. A technician can administer it rapidly and it requires little training and no clinical judgment. It is scored objectively and is able to distinguish the cognitive ability between ill and healthy people during aging by evaluating cognitive areas typically compromised in AD (e.g. verbal fluency and time orientation) (Leifer, 2003).

b. *Laboratory tests*

Using laboratorial tools it is possible to analyze the CSF and its proteins. AD in early stages may cause changes in CSF levels of Aβ. This test does not provide a clear diagnosis of the disease because the reference values of Aβ are not consensual in many clinics. The Aβ levels can also be measured in blood analysis where the concentration levels of Aβ (1-42) peptide are measured in the CSF, and a highly significant reduction of its concentration is

shown in AD patients compared to controls patients (Lesné et al., 2013). It has been suggested that reduced levels of Aβ (1–42) in the CSF are caused by reduced clearance of Aβ from the brain to the blood or to the CSF, as well as enhanced aggregation and plaque deposition in the brain (Humpel, 2011).

c. *Neuroimaging techniques*

Typically these techniques are not used to ensure the diagnosis but to exclude other causes of dementia. The most used technique is the structural imaging like computed tomography (CT) or magnetic resonance imaging (MRI). One example of the use of these techniques is to exclude clinically significant structural lesions such as subdural hematoma and hydrocephalus (Leifer, 2003).

A different approach of neuroimaging is functional imaging. This technique reveals how cells in various brain regions are working by showing how actively the cells use sugar or oxygen. Functional techniques include positron emission tomography (PET) and functional MRI (fMRI). PET is a relatively noninvasive procedure that measures cerebral metabolic rates. Patients with AD have shown reduced use of cerebral glucose that begins in the parietal and temporal regions and later involves the prefrontal cortices (Johnson et al., 2013). More recently other molecules were admitted in PET scans. Radioactive diagnostic agents, like flutametamol F18 and florbetaben F18, estimate the Aβ neurotic plaque density in adult patients with cognitive impairment who are being evaluated for AD and other causes of cognitive decline (Nordberg, 2015). Although this method can provide important information about the presence of amyloid plaques in the brain, it cannot be used for diagnosis purposes because of the presence of amyloid plaques in the brains of people with and without symptoms for AD (Richards & Sabbagh, 2014). Although PET scans cannot be used as a definitive diagnostic tool for AD, they are a very useful method to distinguish AD from other dementias with a fairly high level of accuracy.

Another technique of brain imaging is molecular imaging, which uses highly targeted radiotracers to detect cellular or chemical changes linked to specific diseases. Molecular imaging technologies include single photon emission computed tomography (SPECT) which uses a nuclear isomer emitting gamma rays that can be detected by a gamma camera. Because blood flow in the brain is tightly attached to local brain metabolism and energy use, the tracer is used to assess brain metabolism regionally, in an attempt to enable a diagnose (Matsuda, 2007).

Although these technologies provide enough information about the condition of the patient and whether he or she suffers from the disease, none of these technologies are 100 % certain. Sometimes the patient is diagnosed long after the disease has begun to establish, and the symptoms are already very severe. An early diagnosis would certainly allow for a better quality of life with control of progression of the disease. New technological tools have been tested as the use of nanotechnology or the use of bacteriophages that could detect the disease-related biomarkers. After being identified, it will be possible to study the behavior of those biomarkers that may reveal unknown aspects of the disease (Frenkel & Solomon, 2002; Nazem & Mansoori, 2008).

1.1.4 AD Treatment

No direct treatment is available for AD. Currently, treatment only consists in the administration of drugs that help control the symptoms of dementia. There are now two classes of drugs approved for the symptomatic treatment of AD: (i) cholinesterase inhibitors (ChEIs) like tacrine, the first approved by Food and Drug Administration (FDA) (Schneider, 2013), donepezil, rivastigmine and galantamine and (ii) memantine.

The neurotransmitter acetylcholine plays an important role in the central nervous system (CNS). ChEIs drugs stop or inhibit enzymes from breaking down acetylcholine when it travels from one cell to another. This means that acetylcholine, which is in short supply in AD patients, is not destroyed so quickly and there is more chance of being passed on to the next nerve cell. ChEIs result in higher concentrations of acetylcholine, leading to increased communication between nerve cells, which in turn may temporarily improve or stabilize the symptoms of dementia. The ChEIs are generally well tolerated, although gastrointestinal adverse effects such as nausea, diarrhea and vomiting are the most common adverse effects, and may lead to discontinuation of treatment for some patients (Parsons et al., 2013).

Memantine is a voltage-dependent, moderate-affinity, uncompetitive N-methyl-D-aspartate (NMDA) receptor antagonist that blocks the effects of pathologically elevated levels of glutamate that may lead to neuronal dysfunction. Common undesirable effects are dizziness, headache, constipation, somnolence and hypertension (Matsunaga et al., 2015; Waldemar et al., 2007).

New research has been done in an attempt to create a treatment interacting with protein Aβ. Knowing that Aβ are fragments of APP caused by cleavage of β -secretase and γ -secretase,

the possible creation of inhibitors of these two enzymes would result in the reduction of Aβ and prevent Aβ -mediated downstream neurotoxic events, representing an attractive strategy to combat AD (MacLeod et al., 2015; Wu & Zhang, 2009). Preventing the formation of the presumed toxic oligomeric aggregates of Aβ by small molecules, represents another promising approach for the development of a treatment. For example, zinc ions may be involved in the mediation of Aβ aggregation and toxicity, by reducing its levels in the brain will help decrease the aggregates of Aβ (Miller et al., 2010). More recent studies show promising results in interaction with aggregated Aβ. In these trials, patients were treated with a drug called aducanumab. This drug is a human monoclonal antibody that selectively targets aggregated Aβ. More tests are needed but aducanumab is shown to enter the brain, bind parenchymal Aβ , and reduce soluble and insoluble Aβ in a dose-dependent manner (Sevigny et al., 2016).

Although all these treatments are promising, the biggest bottleneck in the development of therapies and diagnostics for CNS diseases is the presence of the brain barriers (Gao, 2016). There are three important barriers protecting the brain from the entrance of several elements: (i) the choroid plexus epithelium, which is responsible for the secretion of CSF and separates the blood from ventricular CSF, (ii) the arachnoid epithelium separating the blood from the subarachnoid CSF and (iii) the blood brain barrier (BBB), one of the most selective barriers, formed by endothelial cells between blood and brain interstitial fluid (Abbott et al., 2010).

The BBB is the most important barrier in the brain that separates the blood for the CNS. It possesses a unique vascular phenotype that is induced by neighboring cells such as pericytes, astrocytes, and neurons that together form the neurovascular unit. Besides protecting the brain from toxins and pathogens, it is responsible for the homeostatic balance and the selectivity of ions, nutrients and metabolites. One of the hallmarks of the BBB is the restrictive paracellular barrier composed of a continuous network of tight junctions between the endothelial cells (Jones et al., 2014). Only lipophilic molecules can pass through the tight junctions between the endothelial cells (Rooy et al., 2010) such as O_2 and CO_2, which diffuse freely across endothelial cells along with their concentration gradient. The transport of blood-born molecules like drugs and nutrients (for instance glucose and amino acids) is prevented by the endothelial cells requiring the presence of a specific transporter or receptor systems. Conversely, similar mechanisms constitute a way out of the brain for molecules produced by brain cells metabolism (Figure 2) (Ohtsuki & Terasaki, 2007; Zhang & Pardridge, 2001).

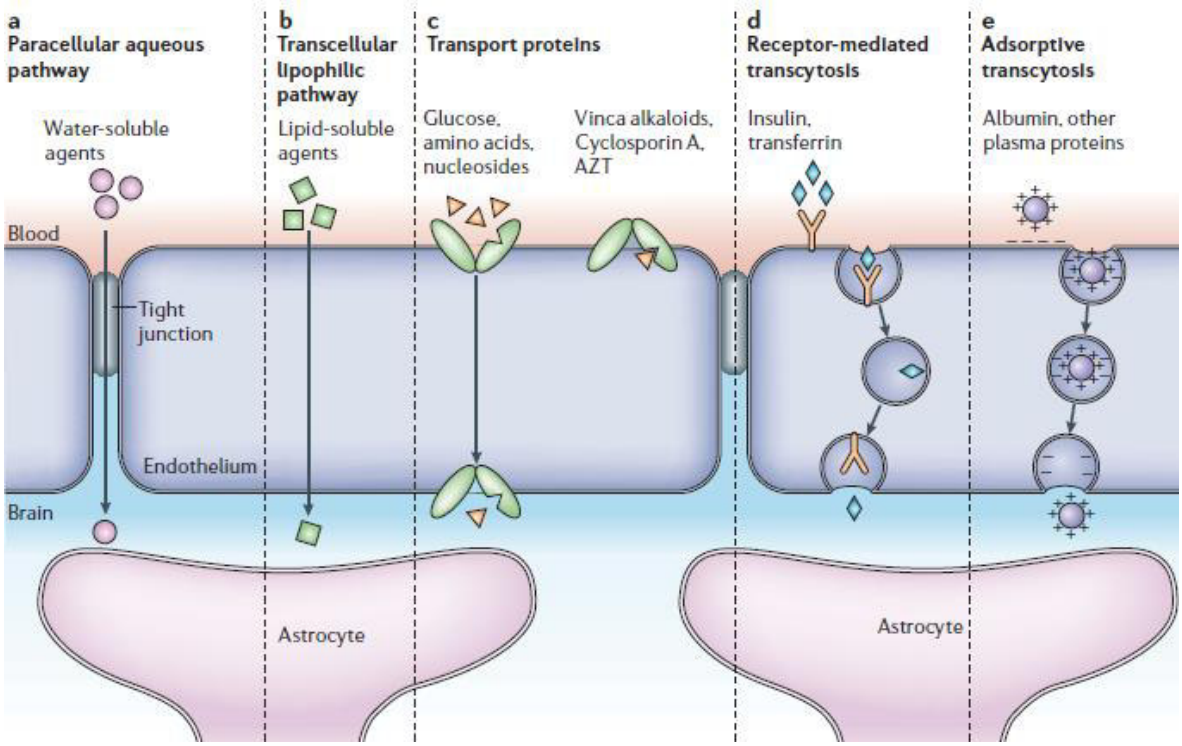

Figure 2 Schematic diagram of the BBB. *Crossing of some molecules through the BBB as well as the transport used* (Abbott et al., 2006).

Some techniques like the use of nanoparticles encapsulated with drugs or virus conjugated with small peptides are already being used to transport to the brain selective particles that target specific biomarkers (J. Li et al., 2012; M. W. Smith et al., 2012). It is known that even when some of this particles reach the brain the most probable is that they are immediately cleared because of the multidrug resistance receptors of endothelial cells (J. V Georgieva et al., 2012).

Among the range of therapeutics for new generation treatments of AD, specific peptide ligands hold a great potential as a tool to selectively target oligomeric/fibrillic Aβ. Recently, Tessier and co-workers reported that a conjugation of small amyloidogenic peptides from the Aβ 42 peptide into the complementarity determining regions (CDR) of a variable domain antibody, generates antibody variants that specifically recognize Aβ soluble oligomers and amyloid fibrils with nanomolar affinity (Perchiacca et al., 2012). The peptide sequences that showed a better affinity for Aβ fibrils and oligomers were those containing the C-terminus of Aβ 30-39 (AIIGLMVGGV) and Aβ 33-42 (LMVGGVVIA). Notably, these small peptide sequences do not recognize plaques which make them the ideal tool to selectively detect the

detrimental forms of Aβ. After the discovery of these peptides it is important to transport then into the CNS, allowing the identification of free Aβ forms.

Taking into account the significant number of people with CNS diseases, it is necessary the development and application of diagnostic/treatment models that specifically target the biomarkers of each disease. The use of bacteriophages arises as a safe, convenient and relatively inexpensive mediator for the transport of peptides to the brain, such as those that recognize Aβ oligomers (Prisco & de Berardinis, 2012; Rakover et al., 2010).

1.2 Bacteriophages

Bacteriophages (or phages for short), are viruses that infect only bacterial cells, a very important characteristic because they won't be harmful to animal cells. Unlike antibiotics therapy, phage therapy is much more specific due to the need of specific receptors on the surface of the host cell. These receptors are only present in some types of bacteria which avoids the destruction of beneficial bacteria in the organism like those present in the microflora (Drulis-Kawa et al., 2012).

Phages genomes consist of either double- or single-stranded DNA or RNA and can be circular or linear. The most extensively studied phages are T4, λ , P1 and M13 which are often used in the treatment of bacterial infections in food and in animal models (Harper, 2011). Although they are very different, these phages have something in common, their structure. It consists of a protein capsid which is produced by the phage, surrounding the phage genome. To replicate they must be capable to recognize the bacteria and then insert their genome into the bacterial cytoplasm. After replication they kill the bacterial host – lytic phages, or they just slow down the bacterial growth using some of its resources weakening it but not destroying it – lysogenic and filamentous phages (Farr et al., 2014).

One of the most used filamentous phage is the M13 phage. This phage has been often used for phage display technique (J. Li et al., 2012), cell imaging (Jin et al., 2014) and drug delivery (Ngweniform et al., 2009).

1.2.1 The M13 filamentous phage

M13 is a long, thin, small size and elongated filamentous phage with of ≈ 880 nm in length and with a diameter of 6.6 nm. Its easy manipulation and the strong fundamental understanding of its biology, makes this phage an interesting platform for diagnose/treatment purposes (Ghosh et al, 2012a).

There are two major characteristics of filamentous phages that makes them suitable to use in humans. First, phages cause no harm to human cells (Kelly et al., 2006; Moon et al., 2015; Pranjol & Hajitou, 2015). Second, M13 is able to bypass the BBB. Frenkel and co-workers (Frenkel & Solomon, 2002), described that the M13 phage is capable to reach the brain via intranasal administration through the olfactory route. The olfactory receptor neurons, present in the nasal cavity, have the capacity of projecting molecules to the first synapse of the olfactory pathway in the olfactory bulb of the brain through their axons. More recently, Ksendozvsky and collaborators (Ksendzovsky et al., 2012), used the convection-enhanced delivery (CED) method to distribute phage M13 in the brain using a pressure gradient, forcing the phage particle to reach the brain.

a. *M13 brain administration*

In order to reach the brain the phage needs to be administered. The use of cocktails of lytic phages has been used for the treatment of bacterial infections. There are several forms of phage administration such as oral, intradermal, intranasal, intravenous among others (Hashiguchi et al., 2010; Kropinski, 2006). Recently, an *in vivo* assay showed that intranasal administration of phages like M13, can rapidly accumulate in different brains zones of mice (Dor-On & Solomon, 2015). Intranasal administration seems to form a highway by which viruses or other transported substances may gain access to the CNS (Solomon, 2008).

Previously, many treatments against bacterial infections using phages were performed. In these studies, phage concentrations on the order of 10^8 have shown to be effective (Chhibber & Kumari, 2012). Even when animals were injected with highest phage concentrations, the revealed secondary effects were very tenuous, showing symptoms as weight loss on 2-6 % of the animals. Additionally, this tests did not presented levels of toxicity or showed to be harmful for humans (Seow et al., 2010).

Although the use of phages is a promising tool, it is necessary to take into account how the immune system acts once the phages are administrated. One of the biggest obstacles is the

fact that the immune system recognizes the phages and automatically acts expelling them from the body (Hashiguchi et al., 2010). Further studies are needed to find out how the phage M13 can be kept longer in the body of patients. Approaches such as the conjugation of phages with sugars and amino-related coating like PEGylation, reduced the immune response. These molecules "mask" phages and reduce the stimulation of the immune system , keeping the phage inside the human body for longer periods (Vaks & Benhar, 2011).

b. *M13 Structure*

The M13 phage contains a circular ssDNA genome encoding a total of 11 proteins. The major coat protein is the P8, with ≈ 50 amino acids and 2,700 - 3,000 copies. Together, with approximately 5 copies each, are four minor capsid proteins P3, P6, P7 and P9, which are located at the ends of the particle (Figure 3).

While P6 has a role in adsorption and morphogenesis, P7 and P9 are required for phage packaging/assembly. Three nonstructural phage proteins, P1, P4 and P11 have a role in phage maturation. P2 and P10 are essential to the DNA synthesis during the phage infections regulating the number of double stranded genomes in the bacterial host. P5 competes with double stranded DNA formation by sequestering copies of the + stranded DNA into a protein/DNA complex destined for packaging into new phage particles (Rakonjac et al., 2011).

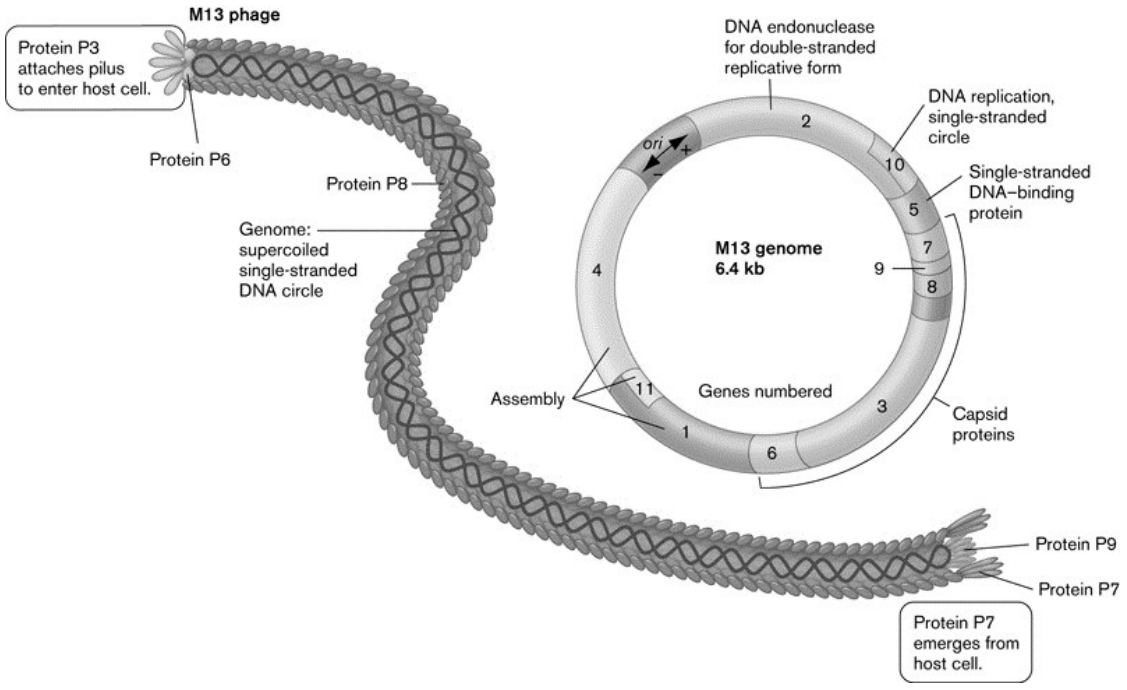

Figure 3 The M13 phage structure and genome
(from:http://www.wwnorton.com/college/biology/microbiology2/ch/11/etopics.aspx)

Programmable protein functionalities promise the ultimate flexibility in assembling heterofunctional nanostructures, which makes this viral system an attractive template for synthesis and assembly of various materials and structures.

The most widely used protein for expression of peptide sequences is P3, a protein that plays an essential role in the penetration of the viral genome into the bacterial host via pilus retraction. During the initial step of infection, P3 mediates adsorption of the phage to its primary receptor, the tip of the host F-pilus. Subsequent interaction with the host entry receptor tolA induces penetration of the viral DNA into the host cytoplasm. This protein has three functional autonomous domains (D1, D2 and D3) joined by glycine rich linkers. The D1-domain at the N-terminus is responsible for the translocation of the viral DNA, the D2-domain binds to the bacterial F-Pilus and the C-terminal, and the D3-domain is essential for the assembly of a stable capsid. For expression of the proteins on the surface of the phage, the polypeptides are linked to the N-terminal of P3, and not to the C-terminal, to allow phage assembly (Y. Georgieva & Konthur, 2011).

1.2.2 M13 Phage Genetic Manipulation

The interest in the use of phages as a therapeutic/diagnostic tool appeared some years after George Smith developed the method of phage display (G. P. Smith, 1985). It is a molecular technique used for identifying peptides with high affinity and specificity interactions towards a wide spectrum of targets. The DNA that encodes a given polypeptide is fused with the phage genome, and the desired protein is expressed on the surface of the phage particle (Hairul Bahara et al., 2013; Vargas-sanchez et al., 2016).

The ability to genetically modify phages brought a new range of therapies for different diseases. The basis of the therapy is to modify the phage coat protein P3 with small copies of peptide sequences, which are then expressed on the surface of the phage and used to identify biomarkers of certain diseases. These recombinant phages show many advantages against the use of other therapeutic systems like drugs or chemotherapy. They have high levels of purity, great specificity in relation to the target and when administered to animals show no evidence of toxic effects (Drulis-Kawa et al., 2012; Kutter et al., 2010; Loc-Carrillo & Abedon, 2011).

Studies already demonstrate the use of M13 for application in cancer cell imaging. In this case they genetically modified M13 by displaying a sequence in the P3 protein that has affinity to collagen and displaying streptavidin binding peptide (SBP) on P8. SBP allows

binding to streptavidin-conjugated molecules for imaging or for use as therapeutic agents. With SBP the phage can be tracked and located by imaging techniques (Jin et al., 2014).

With the current knowledge about the biomarkers of some neuronal diseases, it is necessary to create a tool for their identification. Considering this possibility, studies involving the display on M13 coat proteins of peptides capable of identifying the Aβ have shown promising results. A study shows the display of a novel Ɗ -amino acid peptide, which binds specifically to Aβ, called "Ɗ -pep" or "D1". This peptide is used on transgenic mice to inhibit amyloid plaque formation and cell toxicity (Van Groen et al., 2013). Other peptides have been displayed with the purpose of slowing Aβ accumulation. Often these peptides did not act on the amyloid plaques but on its oligomeric and monomeric form, thereby preventing their accumulation (Kawasaki et al., 2011; Rudolph et al., 2016).

1.2.3 M13 Phage Chemical Functionalization

In applications where a large loading capacity is desired, such as a fluorochrome or a drug, it is common to label the major coat protein P8 due to its high copy number. To extend the scope of phage applications, this protein is chemically functionalized and not genetically manipulated like the P3 protein. This happens because the P8 can only tolerate the incorporation of 6–8 amino acids (Hess et al., 2012). Strategies involving P8 functionalization have been employed to incorporate a wide range of functional groups, including synthetic chemical compounds (Bernard & Francis, 2014; Chung et al., 2014; Ghosh et al., 2012b).

Some studies already demonstrate phage functionalization with drugs as doxorubicin (DOX) for targeted drug delivery for tumor cells (Ghosh et al., 2012a), or fluorescent molecules that allowed the use of the M13 phage in cancer cell imaging (K. Li et al., 2010).

The construction of a phage particle expressing peptide ligands, able to identify typical AD biomarkers, as well as flourishing molecules, allows the creation of a new platform for AD diagnosis.

1.3 Motivation and Objectives

The numbers of patients with AD are increasing and today there are around 47 million people worldwide suffering with AD, with estimations of 131 million people affected by the year 2050. The motivation for this thesis born with the necessity to create a diagnostic tool to allow an early detention of AD, an important step not only to increase the quality of life of AD patients, but also for a cost reduction with heath care systems and treatments. The ability to provide an accurate and early diagnosis will bring some advantages like knowing which factors are responsible for AD, avoid misdiagnosis and improve the patient's life knowing what to expect in the future. Moreover, it will provide a wide range of opportunities for the development of new forms of treatment as well as the development of new drugs.

The main objective of this project was to develop a bacteriophage-based platform for early diagnosis of Alzheimer's disease. To achieve that goal two main starting points were taken into consideration, the ability of the M13 bacteriophage to cross the BBB and the existence of peptide sequences able to specifically recognize Aβ fibrils and oligomers. The M13 phage was genetically modified in order to display on its surface peptide ligands which recognize Aβ fibrils and oligomers. In addition to genetic modification, the phage was chemically functionalized with a fluorochrome to allow tracking of the phage particles in for future *in vivo* studies.

2. MATERIALS AND METHODS

2.1 M13KE Production and DNA Extraction

2.1.1 *Escherichia coli* Culture

During the work, two different *E. coli* strains were used (Table 2).

Table 2 E. coli strains.

Strain	Genotype	Origin
ER2723	F´*proA+B+ lacIq Δ(lacZ)M15 zzf::Tn10(TetR)/ fhuA2 glnV Δ(lac-proAB) thi-1 Δ(hsdS-mcrB)5*	New England Biolabs (Ref. E4104)
JM109	F´ *traD36 proA+B+ lacIq Δ(lacZ)M15/ Δ(lac-proAB) glnV44 e14- gyrA96 recA1 relA1 endA1 thi hsdR17*	New England Biolabs (Ref. E4107)

For daily uses, both strains were cultured in 3-5 ml of Lysogeny Broth (LB) broth (25 g/l, NzyTech) medium in a 15 ml falcon tube for 5-6 hours, at 37 °C with and 200 rpm. For strain ER2738, tetracycline (Sigma-Aldrich Co. LLC, 87128) was added to the medium to a final concentration of 20 mg/ml. The strains were also maintained and weekly renewed in solid culture in LB agar plates [LB broth with 20 g/l of agar (LiofilChem, Frilabo)], supplemented with 20 mg/ml of tetracycline for the ER2738 strain.

2.1.2 M13KE Phage Stock Production

The M13KE phage was obtained by two methods:

a) an inoculum of 20 ml of LB medium with 150 µl of an overnight *E. coli* culture, 1 µl of M13KE phage (New England BioLabs® Inc, N0316S) and 75 µl of magnesium chloride [($MgCl_2$), VWR] were allowed to grow for 5 hours, at 37 ºC and 200 rpm. Then, the inoculum was centrifuged (Thermo Scientific – CL31R Multispeed) and the supernatant filtered with a

0.2 µ m polyethersulfone (PES) filter (Fiorini, 6002S) to a 15 ml tube. The phage solution was stored at 4 °C.

b) An inoculum of 20 ml of LB medium with 200 µl of an overnight *E. coli* culture and 1 µl of M13KE phage was allowed to grow for 4-5 hours, at 37 ºC and 200 rpm. In order to remove the bacterial cells, the solution was centrifuged at 6500 rpm for 10 minutes. The supernatant was transferred to a fresh tube and another centrifugation was conducted. Sixteen ml of supernatant was transferred to a new tube and 4 ml of 20 % PEG/NaCl [polyethyleneglycol-8000 (PEG_{8000}) (w/v) (Fisher Scientific)/ 2.5 M sodium chloride (NaCl, Panreac)] were added. Afterwards, the solution was briefly mixed and the phage was allowed to precipitate for 1 hour or overnight at 4 °C. To obtain phage pellet the solution was centrifuged at 13000 rpm for 15 minutes. The supernatant was discarded and the pellet resuspended in 1 ml Tris-buffered saline [(TBS): 50 mM Tris-base pH 7.5 and 150 mM NaCl)]. Then the supernatant was transferred to an eppendorf tube. Then, 200 µl of a PEG/NaCl solution were added to the tube and incubated on ice for 15-60 minutes. The solution was centrifuged at 13000 rpm for 10 minutes and the supernatant discarded. To remove remaining supernatant a spin was performed. Finally the pellet was dried at room temperature for 30 min, resuspended in 200 µl of TBS and stored at 4 °C.

2.1.3 M13KE Phage Quantification

M13KE phage quantification was performed by plaque forming units (PFUs) assay. This method is only possible because of the use of X-gal (5-bromo-4-chloro-3-indolyl-β -D-galactoside) and IPTG (isopropyl β -D-1-thiogalactopyranoside). This technique uses the lacZα operon present in M13KE vector plus the complementary lacZ omega fragment of the *E. coli* strain used as host. This operon has the ability to produce galactosidase. The presence or absence of this protein can easily be determined through the use IPTG. IPTG is the lacZ gene inducer and is necessary for the production of the galactosidase. The usual substrate for the lacZ gene protein product is galactose, which is metabolized into lactose and glucose. X-Gal is a colorless, modified galactose sugar that when metabolized by galactosidase results in a product of bright blue color. This method allows the visualization of phage in plaques – blue plaques.

Using a 96-well plate (Fisher Scientific), several phage dilutions were made adding 90 µl of saline magnesium (SM) buffer [100 mM NaCl, 8 mM magnesium sulfate heptahydrate

($MgSO_4$, Panreac) and 50 mM Tris-HCl pH 7.5 (Sigma)], on each well plus 10 µl of phage solution on the first well. In the succeeding wells 10 µl of the previous dilution were added. For plating, 10 µl of each dilution was plated on LB/IPTG/X-Gal agar plates [LB agar plates supplemented with 0.05 g/l X-Gal and 0.25 mM IPTG (both from NzyTech)] covered with an *E. coli* lawn (100 µl of an overnight culture) plus 3 ml of LB Top-agar (LB with 0.7 % of agar). Drops were allowed to dry and plates were incubated overnight at 37 ºC (Figure 4).

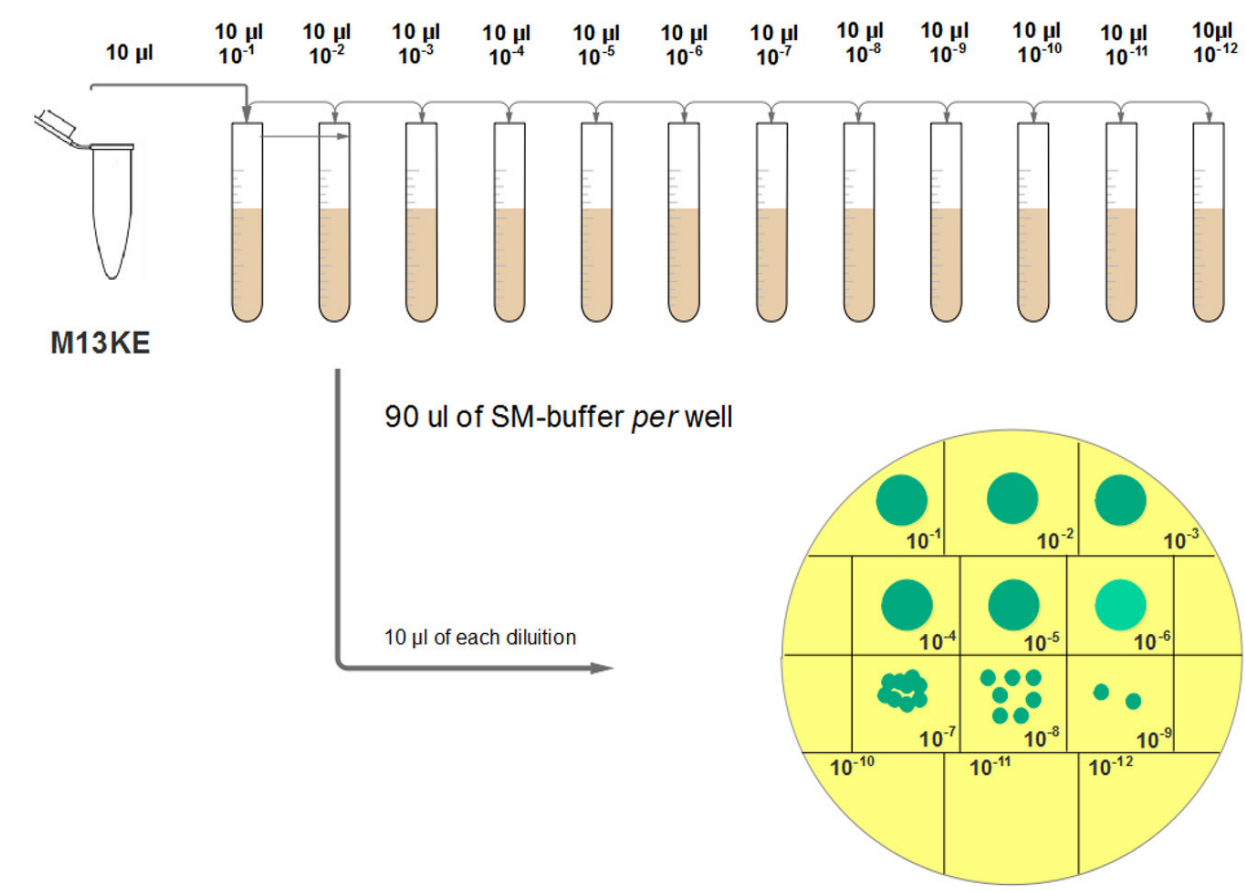

Figure 4 Phage quantification protocol.

After incubation, infectious phage particles were counted on the plate(s) containing 3-100 isolated blue plaques. Phage titer was calculated using the following equation (1).

$$M13KE\left(\frac{pfu's}{ml}\right) = \frac{number\ of\ bue\ plaques\ \times\ diluation\ factor}{drop\ volume\ (ml)}$$

2.1.4 M13KE Phage dsDNA extraction

The M13KE phage dsDNA was obtained by two methods:

a) 100 µl of M13KE were inoculated with 100 µl of an overnight *E. coli* culture in 10 ml of LB for 5 hours. One ml of the cellular suspension was centrifuged at 1300 rpm and the supernatant was discarded. Another 1 ml was added to the pellet and the centrifugation process was repeated. The supernatant was discarded, 200 µl of cold extraction solution P1 [50 mM glucose (Liofilchem®), 10 mM ethylenediamine tetraacetic acid (EDTA, Fluka Analytical, Sigma) and 25 mM Tris-base pH 8.0] were added to the pellet and the solution was mixed to dissolve the pellet. Then, 400 µl of fresh extraction solution P2 [0.2 M sodium hydroxide (Sigma-Aldrich Co. LLC) and 1 % sodium dodecyl sulfate (SDS, Fisher Scientific] were added and the tube was repeatedly and slightly inverted. For DNA precipitation, 300 µl of cold extraction solution P3 [3 M potassium acetate (Fisher Scientific) and 11 % acetic acid] were added and the tube inverted several times. The tube was incubated for 10 minutes on ice and centrifuged for 5 minutes at 13500 rpm. The supernatant was carefully transferred to another tube containing 0.5 ml of absolute ethanol (Fisher Scientific). The tube was stirred in a vortex and incubated at -20 °C for 10 minutes. Afterwards, the solution was centrifuged for 5 minutes at 13500 rpm and the supernatant discarded. The pellet was washed with 1 ml of 70 % ethanol and mixed. The centrifugation process was repeated and the supernatant carefully discarded. The pellet was allowed to dry at 42 °C and finally dissolved in 20 µl of Tris/EDTA (TE) buffer [0.1 M Tris-base (Fisher Scientific) and 10 mM EDTA].

b) 10 µl of M13KE were inoculated with 100 µl of an overnight *E. coli* culture in 10 ml of LB medium for 4-5 hours. After incubation the DNA was extracted using the plasmid extraction kit - NucleoSpin® Plasmid (Macherey-Nagel), following the manufacturer instructions.

In both cases the DNA concentration was measured in a NanoDrop1000 Spectrophotometer (Thermo Scientific).

2.2 Cloning Procedure

With the purpose to create a phage particle able to express the peptide sequence of interest on its surface, the DNA sequence (insert) encoding the peptide of interest, was cloned

into the gene 3 of the M13KE genome (vector). This manipulation was carried out through a digestion/ligation protocol. Two different inserts were used, the Aβ 30-39 (AIIGLMVGGV) and the Aβ 33-42 (GLMVGGVVIA). These inserts were obtained using two different methodologies, (see sections 2.5.1 and 2.5.2).

2.2.1 DNA Double-Digestion

Before cloning the inserts into the vector, both vector and inserts DNA were double digested using the high-fidelity enzymes EagI-HF (New England BioLabs® Inc., R3505S) and KpnI-HF (New England BioLabs® Inc., R3142S). These enzymes cut at 1614 bp and 1630 bp respectively on the N-terminal of gene 3 of the M13KE vector and at the ends of the Aβ inserts, producing sticky ends (Figure 5).

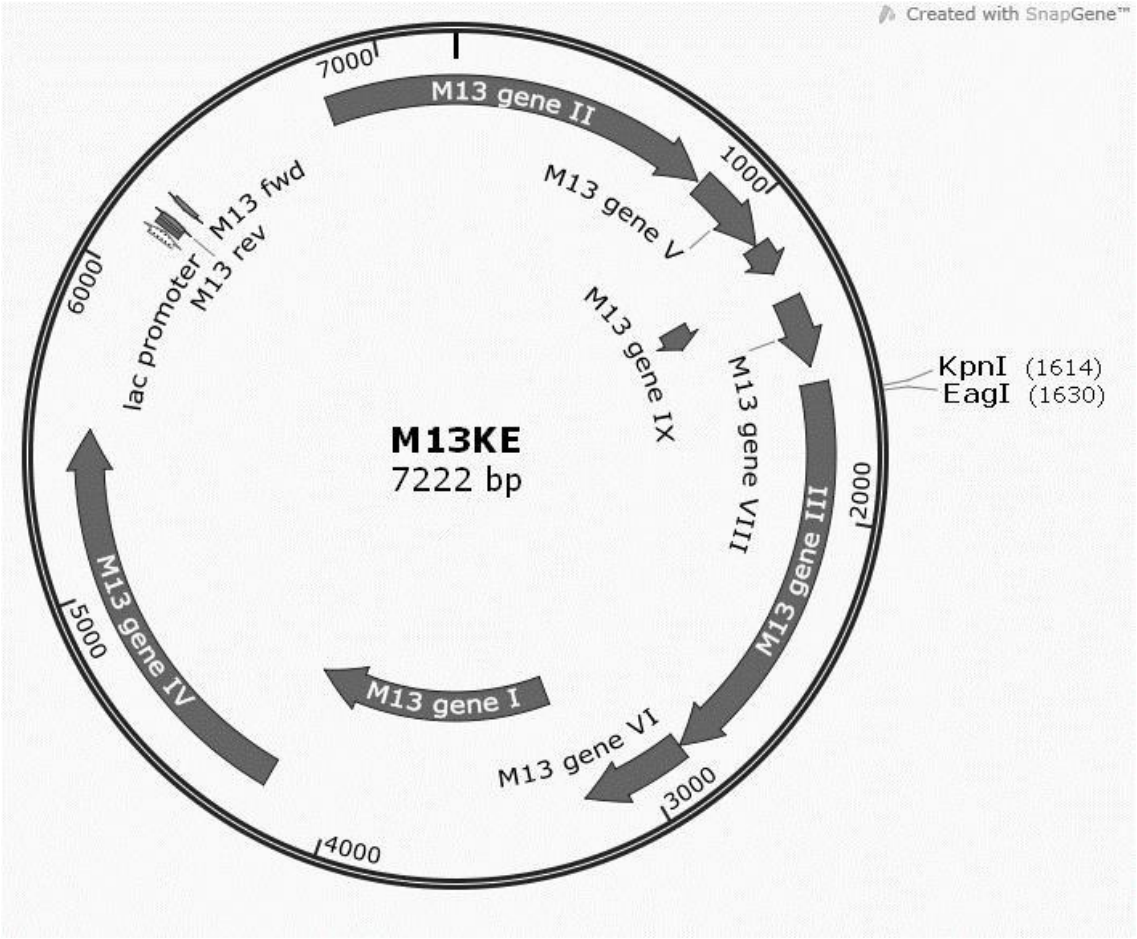

Figure 5 M13KE genome map. *Images were obtained using the SnapGene software (from GSL Biotech).*

The used enzymes are unique cutters that allow the introduction of the insert in the gene 3 of the phage, with the consequent display of the peptide at all the 5 copies of the phage P3 minor coat protein.

Each digestion was performed in a total volume of 20 µl by mixing 1 µl of each enzyme, 2 µl of CutSmart™ buffer (NewEngland BioLabs® Inc, B7204S), the equivalent of 500 ng of DNA for the M13KE and nuclease free water (NzyTech). The inserts were digested using different concentrations of DNA, according to the respective approach of insert synthesis. The mixtures were incubated at 37 ºC during 2-5 hours and then 20 minutes at 65 ºC to inactivate enzymatic activity.

2.2.2 Vector::Insert Ligation

Due to the different sizes and molarities of the vector and the inserts it was necessary to calculate the quantities necessary to perform the ligation using the following equation (2).

$$required\ mass\ insert\ (g) = \ desired\ \frac{insert}{vector}\ molar\ ratio\ x\ mass\ of\ vector\ (g) x\ \frac{insert}{vector} lengths$$

The ligation protocol was performed choosing a ratio of 3:1 of insert molar excess and 20-100 ng of vector. The ligation of the M13KE vector with the inserts was carried out using T4 DNA ligase (NewEngland BioLabs® Inc, M0202S). The ligation conditions are represented in Table 3.

Table 3 Reaction conditions for ligation protocol.

Linear vector DNA	**20-100 ng**
Insert DNA	3:1 molar ratio over vector
10x T4 DNA Ligase buffer	2 µl
T4 DNA Ligase	1 µl
Nuclease free water	Up to 20 µl

The reaction was mixed and incubate overnight at 16 °C. After incubation, T4 DNA ligase was inactivated at 65 °C for 10 minutes. The ligation product was store at -20 °C until bacterial transformation.

2.3 Transformation of bacterial competent cells

The transformation process allows the entrance of the mutated DNA into the host cell. To better evaluate the competence for transformation, two types of competent cells were produced: electrocompetent and chemocompetent cells. Both strains ER2738/JM109 were used.

2.3.1 Electrocompetent Cells Preparation

An inoculum was made by adding 1 ml of the overnight *E. coli* culture to 100 ml of liquid LB medium in a 500 ml Erlenmeyer. The culture was incubated at 37 ºC and 200 rpm until reaching an OD_{600} of 0.35 and then it was chilled on ice. All steps after chilling the cells were performed at 4 ºC and ice-cold 10 % (v/v) glycerol (Fisher Chemical) was used for improved efficiency of the transformation process. The inoculum was divided in 2 tubes of 50 ml and the cells were pelleted by centrifugation at 5000 rpm for 15 minutes at 4 ºC. The supernatant was discarded and each pellet was gently resuspended in 40 ml 10 % (v/v) of glycerol. Another centrifugation was performed at the same conditions and the supernatant discarded. The obtained pellets were resuspended by adding 20 ml of 10 % (v/v) glycerol to each falcon. After resuspended, both suspensions were joined. The centrifugation step was performed twice. In the first, the pellet was resuspended in 20 ml of 10 % (v/v) glycerol and in the second the pellet was resuspended in 10 ml of 10 % (v/v) glycerol. One last centrifugation was performed and the supernatant was discarded. Finally the pellet was resuspended in 200 µl of 10 % (v/v) glycerol and 20 µl aliquots were made and stored at – 80 °C.

a. *Electroporation process*

To transform electrocompetent *E. coli* cells with the vector-insert product, a Gene Pulser Xcell™ Electroporation System was used (Bio-Rad Laboratories, Inc). An aliquot of 20 µl electrocompetent *E. coli* cells was thawed on ice and mixed with 3 µl of the product. The cells were incubated with the DNA for 1 minute on ice and then transferred to a pre-cooled 0.2 mm

cuvette (CellProjects, EP-102). The cuvette was placed in the chamber slide and pulsed with 2.5 kV. The cuvette was removed and 1 ml of super optimal broth with catabolite repression [(SOC), 31.54 g/l, (NzyTech, MB28001)] medium was added to the cells instantaneously. Then the transformants were allowed to grow for 1 hour at 37 °C, 200 rpm. Different volumes of the incubated cells were plated in LB/X-Gal/IPTG plates with: 10 µl, 100 µl and the remaining pelleted cells. The plates were incubated overnight at 37 °C to enable the growth of blue colonies for future amplification of DNA transformants.

2.3.2 Chemocompetent Cells Preparation

An inoculum was made by adding 800 µl of an overnight *E. coli* culture to 80 ml of liquid LB medium in a 200 ml Erlenmeyer. The culture was incubated at 37 °C and 200 rpm until reaching an OD_{600} of 0.45 and then chilled on ice. To improve the efficiency of the transformation process all steps after chilling the cells were performed at 4 °C and ice-cold solutions were used. The inoculum was divided in two 50 ml tubes and centrifuged at 4000 rpm, during 10 minutes at 4 °C. Then each pellet was gently resuspended in 20 ml of ice cold 0.1 M $MgCl_2$. The cells were chilled for at least 30 minutes on ice. Another centrifugation with the same conditions was performed and the supernatant discarded. Then each pellet was gently resuspended in 4 ml of sterile 0.1 M calcium chloride ($CaCl_2$, Panreac) and the content of the two tubes was joined. The solution was again centrifuged and finally resuspended in 800 µl of 0.1 M $CaCl_2$ + 15 % glycerol. Aliquots of 80 µl were made and stored at – 80 °C.

a. *Heat shock process*

To transform chemocompetent *E. coli* cells with the vector-insert product, an aliquot of 80 µl of chemocompetent *E. coli* cells was incubated with 5 µl of the ligation product for 30 minutes on ice. The cells were then subjected to a heat shock by incubating 40 seconds at 42 °C and then for 2 minutes on ice. The transformants were left to recover with 900 µl of SOC medium for 1 hour at 37 °C and 200 rpm. The incubated cells were plated as described in section 2.3.1.

2.4 Cloning Confirmation

2.4.1 Phage Clones Selection

After growing overnight, random blue colonies were picked with sterile tips and inserted into 50 ml falcons with 15 ml of LB medium and 100 µl of an overnight *E. coli* culture and left to grow at 37 °C, for 5 hours at 200 rpm. After incubation the cells were centrifuged at 10000 rpm for 3 minutes and the supernatant was filtered with a 0.2 µ m PES filter. The resulting amplified phage was stored at 4 °C until DNA extraction.

2.4.2 DNA Extraction

For the extraction of ssDNA from each selected clone in section 2.4.1, 500 µl of phage solution was mixed with 200 µl of PEG/NaCl in order to precipitate the phage DNA from the supernatant. After gently inverting, the mixture was left to rest for 15 minutes then centrifuged for 10 minutes at 14000 rpm and the supernatant discarded. After centrifugation the pellet was resuspended in 100 µl of iodide buffer [10 mM Tris-HCl pH 8.0, 1 mM EDTA, 4 M sodium iodide (Riedel Haen)]. Immediately afterwards, 2 volumes of TE buffer were added. Phenol (AppliChem, Frilabo)/chloroform (Fisher Sientific) (50/50: v/v; twice) and chloroform extraction followed by ethanol precipitation were performed. The final pellet was resuspended in 20 µl of TE buffer. After extraction the DNA concentration was measured in a NanoDrop1000 Spectrophotometer.

In order to minimize the negative clones sent for sequencing, amplification of the gene 3 region of the phage, where the inserts were cloned, was performed. The DNA was amplified through a 20 µl PCR reaction using KAPA Taq DNA Polymerase (KAPABiosystems, KR0352) and KAPA dNTP Mix (KAPA Biosytems, KK1017) containing dATP, dCTP, dGTP, and dTTP to complete the amplification.

The used primers were designed in order to flank the sequence where the inserts must be inserted (Table 4). Primers used in this work were synthetized by Invitrogen, ThermoScientific.

Table 4 Primers used to confirm the insertion of Aβ sequences into the phage genome.

Primer	5'- 3' Sequence
Forward (# 237)	5' TTA ACT CCC TGC AAG CCT CA 3'
Reverse (# 98)	5' CCC TCA TAG TTA GCG TAA CG 3'

Table 5 and 6 shows the mix for the PCR reaction and the reaction protocol, following the manufacturer instructions.

Table 5 PCR reaction.

Component	*Per* tube
5X KAPA Taq Buffer	2 µl
10 mM KAPA dNTP Mix	0.4 µl
10 µ M Forward Primer	0.8 µl
10 µ M Reverse Primer	0.8 µl
Nuclease free water	Up to 20 µl
DNA	< 25 ng
5 U/µl KAPA Taq DNA Polymerase	0.8 µl

Table 6 PCR protocol.

Step	Temperature	Time	Cycles
Initial Denaturation	95	30s	1
Denaturation	95	10s	25-30
Annealing	63	30s	
Extension	72	30s	
Final Extension	72	30s	1
Hold	4	Hold	Hold

Following PCR, the DNA fragments length was confirmed by gel electrophoresis, on a 2.5 % agarose (Fisher Scientific) and Tris-acetate-EDTA [TAE: 40 mM Tris-base, 20 mM acetic acid (VWR) and 0.05 M EDTA] gel stained with Thiazole Orange (Sigma – Aldrich Co. LLC). Next, the PCR products were purified using the NucleoSpin® Gel and PCR Clean-up Kit (Macherey-Nagel) following the manufacturer's instructions. The DNA was quantified, in a NanoDrop1000 Spectrophotometer and sent to sequence. A 10 µl reaction was prepared with 20 ng/µl of the cleaned PCR product and 3 µl of the forward primer (#237), at a concentration of 10 mM. The samples were sequenced by Stab Vida.

2.5 M13 Genetic Manipulation

2.5.1 Aβ Sequences Cloning

In this first approach of cloning two different techniques were used to insert the Aβ peptide sequences into the M13 genome.

The first technique was based on the phage display manual from New England Biolabs, following the manufactures instructions (Noren & Noren, 2001). In this technique, an extension primer was annealed with a primer containing the Aβ 30-30 and Aβ 33-42 peptide sequences. To obtain the primers, the amino acid sequences were converted to nucleotide sequences using the specific codons for each amino acid (Table 7). Due to the codon bias, different codons were used for the same amino acid. After annealing, a DNA polymerase provides the extension resulting in the formation of the inserts of interest.

Table 7 Primers sequences to obtain the Aβ sequences. *In red the restriction site of KpnI, in green the restriction site of EagI and in purple the sequence of the peptide of interest.*

Primer Name	5'–'3 Sequence
Extension primer Forward	5' CATGCCCGGGTACCTTTCTATTCTC '3
Aβ 30-39 Reverse	5' CATGTTTCGGCCGAGACACCCCCTACCATGAGACCTATGATAGCA GAGTGAGAATAGAAAGGTACCCGGG '3
Aβ 33-42 Reverse	5'CATGTTTCGGCCGACGCAATTACGACACCCCCTACCATGAGACCA GAGTGAGAATAGAAAGGTACCCGGG '3

Inserts were obtained annealing 5 µ g of the extension primer with 4 µ g of the primer that contains the Aβ sequence, in a total volume of 50 µl TE buffer and 10 mM of EDTA containing 100 mM NaCl.

After heating to 95 °C, the solution was slowly cooled (15-30 minutes) to less than 37 °C in a water bath. To guarantee the extension of the annealing, a mixture of 119 µl of nuclease free water, 20 µl of 10X NEBuffer 2 (NewEngland BioLabs® Inc., B7002S), 50 µl of annealed duplex, 8 µl of 10 mM dNTP's and 3 µl of Klenow DNA polymerase I fragment (NewEngland BioLabs® Inc., M0210S) were incubated at 37 °C for 10 minutes and then at 65 °C for 15 minutes. 4 µl of this solution were stored for later analysis.

To complete the synthesis of inserts, a double digestion was performed by cutting the duplex with EagI and KpnI. Contrary to what was described in section 2.1.1, the digestion was done by mixing 196 µl of the extension reaction, 154 µl of nuclease free water, 40 µl of CutSmart™ buffer, 5 µl of EagI-HF and 5 µl of KpnI-HF. After mixing all components, the solution was incubated at 37 °C for 3-5 hours. The DNA was purified using a phenol /chloroform solution, then extracted with chloroform and finally precipitated with ethanol.

Inserts were confirmed in a 3 % agarose gel in TAE buffer by loading 4 µl of the undigested duplex as well as a low molecular weight DNA ladder (NewEngland BioLabs® Inc, N3233S). The DNA concentration was also measured using the NanoDrop 1000 Spectrophotometer.

The other technique was based on a previous work from Rangel and co-workers (Rangel et al., 2013). In their work they constructed a phagemid particle and inserted it on a cell-penetrating peptide called penetratin. To obtain the insert, an annealing with 2 primers with 100 % complementarity was performed following a heating and cooling protocol. We focused on this technique to design the primers to obtain both Aβ inserts (Table 8).

Table 8 Primers sequences to obtain the Aβ sequences. *In red the restriction site of KpnI, in green the restriction site of EagI and in purple the sequence of the peptide of interest.*

Primer	5'- 3' Sequence
Aβ 30-39 Forward	5' GCCCCGGGTACCGCTATCATAGGTCTCATGGTAGGGGGTGTCCGGCCGGCCCCG '3
Aβ 30-39 Reverse	5'CGGGGCCGGCCGGACACCCCCTACCATGAGACCTATGATAGCGGTACCCGGGGC 3'
Aβ 33-42 Forward	5' GCCCCGGGTACCGGTCTCATGGTAGGGGGTGTCGTAATTGCGCGGCCGGCCCCG 3'
Aβ 33-42 Reverse	5'CGGGGCCGGCCGCGCAATTACGACACCCCCTACCATGAGACCGGTACCCGGGGC 3'

Equimolar amounts of each primer (2 µ g of DNA) were mixed and the final volume was adjusted to 50 µl with 10 mM Tris-HCl pH 8.0. The annealing was achieved performing the protocol showed in Table 9 in a MyCycler™ Thermal Cycler (Bio-Rad Laboratories, Inc.). The inserts were stored at -20 °C until usage.

Table 9 Protocol for primer annealing.

Temperature	93 °C	80 °C	75 °C	70 °C	65 °C	40 °C	4 °C
Time (minutes)	3	20	20	20	20	60	∞

Before carrying out the digestion, the inserts were confirmed in a 3 % agarose gel and the DNA concentration measured with NanoDrop1000 Spectrophotometer. After confirmation, the digestion of the two inserts was performed like described in section 2.1.1 but the used DNA amount of each insert was 200 ng.

2.5.2 Round PCR

This second approach is a PCR-based mutagenesis technique (Liu & Naismith, 2008). In this technique the phage M13KE DNA was not modified through a digestion/ligation protocol but altered during DNA amplification process. In this technique one of the primers that amplify the M13 DNA contains the Aβ peptide sequence in its beginning, and the other primer was designed in order to obtain a phosphorylated end, so that the PCR product could be re-circularized into a circle and used in the transformation process. Figure 6 represents schematically the principle of the technique.

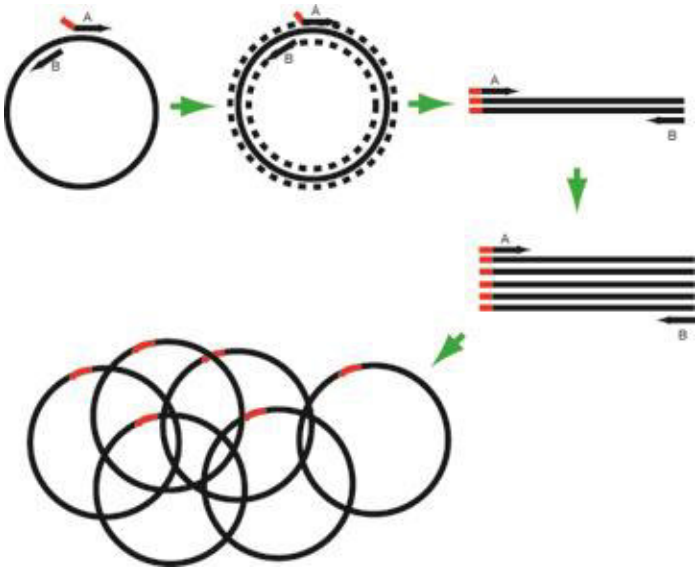

Figure 6 Round PCR. ***A*** *– Primer with the Aβ sequence.* ***B*** *– Phosphorylated primer (from: http://openwetware.org/wiki/' Round-the-horn_site-directed_mutagenesis)*

The sequences of the primers are represented in Table 10. The universal primer is common to both the Aβ peptides primers and corresponds to the phosphorylated primer (Figure 6B).

Table 10 Used primers in the Round PCR technique. *In red the restriction site of KpnI, in green the restriction site of EagI and in purple the sequence of the peptide of interest.*

Primer	5'- 3' Sequence
Universal Primer	5' GTGAGAATAGAAAGGTACCACTAAAGG '3
Aβ 30-39	5'GCTATCATAGGTCTCATGGTAGGGGGTGTATCGGCCGAAACTGTTGAAAG 3'
Aβ 33-42	5´GGTCTCATGGTAGGGGGTGTCGTAATTGCGTCGGCCGAAACTGTTGAAAG 3´

For DNA amplification a 25 µl PCR reaction was made using KAPA HiFi DNA Polymerase (1 U/µl) (KAPABiosystems, KK2102). The reaction conditions are represented in Table 11 and the PCR protocol in Table 12.

Table 11 General KAPA HiFi master mix.

Component	
Nuclease free water	Up to 25 µl
5X KAPA HiFi Buffer	5 µl
10 mM KAPA dNTP Mix	0.75 µl
10 µ M Forward Primer	0.75 µl
10 µ M Reverse Primer	0.75 µl
Template DNA	10 ng

Table 12 PCR protocol.

Step	Temperature	Time	Cycles
Initial Denaturation	98	30s	1
Denaturation	98	10s	25-30
Annealing	67.1	30s	
Extension	72	3 min 40s	
Final Extension	72	10 min	1
Hold	4	Hold	Hold

After the PCR protocol, 4 µl of the PCR product was run in a 1 % agarose gel as well as 4 µl of 1 kb DNA ladder (New England Biolabs® Inc, N3232S). After gel confirmation, the PCR product was purified using a PCR product cleaning kit.

a. *Vector re-circularization*

To allow the transformation of the vector into competent cells a ligation was performed in order to re-circularizate the vector. A 20 µl reaction was done using T4 DNA ligase. The ligation conditions are presented in Table 13.

Table 13 Re-circularization of the vector.

Linear vector DNA	20-10 ng
10x T4 DNA Ligase buffer	2 µl
T4 DNA Ligase	1 µl
Nuclease free water	Up to 20 µl

The reaction was mixed and incubated overnight at 16 °C. After incubation, T4 DNA ligase was inactivated at 65 °C for 10 minutes. The ligation product was stored at -20 °C until the transformation process.

2.5.3 Phagemid Cloning System

The third and last approach used in this work consisted in the construction of a phagemid particle which is a cloning system using an ampicillin resistant plasmid, pETDuet-1 (Addgene, 71146), and the kanamycin resistant M13KO7 helper phage (NewEngland BioLabs® Inc, N0315S), a derivative of the M13 phage.

Basic components of a phagemid mainly include the replication origin of a plasmid, the selective marker (antibiotic resistance usually), the intergenic region (IG region, usually contains the packing sequence and replication origin of minus and plus strands), a gene of a phage coat protein, restriction enzyme recognition sites, a promoter and a DNA segment encoding a signal peptide (Figure 7) (Qi et al., 2012).

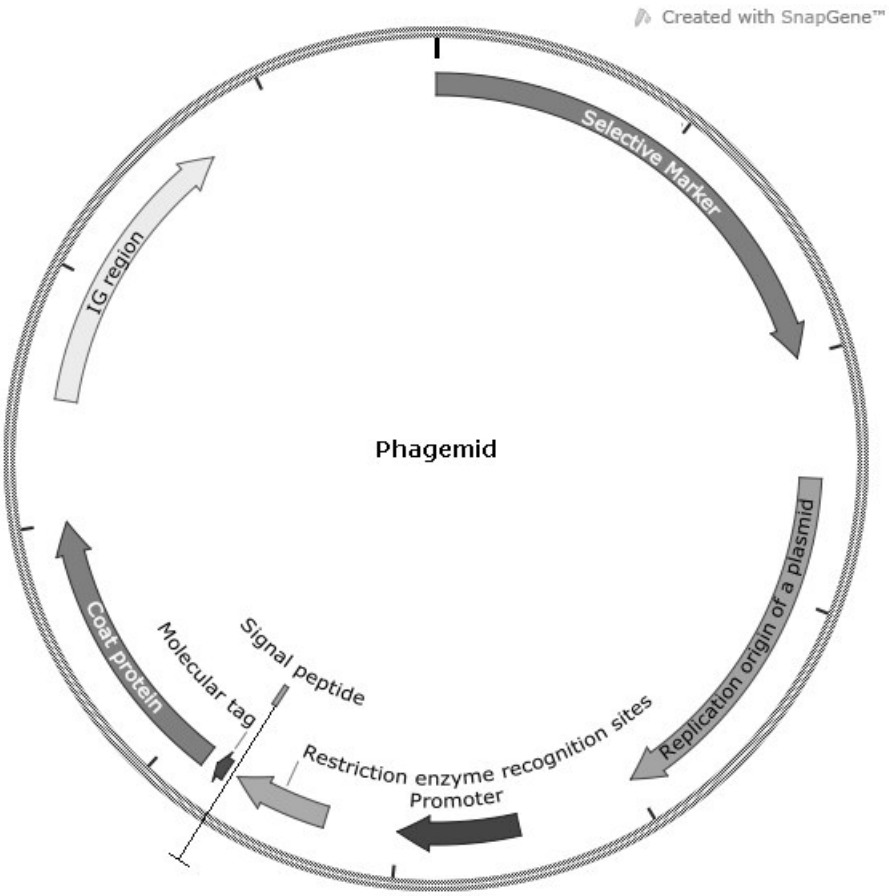

Figure 7 Scheme of a general phagemid structure.

Phagemids can be converted to filamentous phage particles with the same morphology by co-infection with helper phages such as M13KO7.

The construction of the phagemid can be divided into different steps (Figure 8).

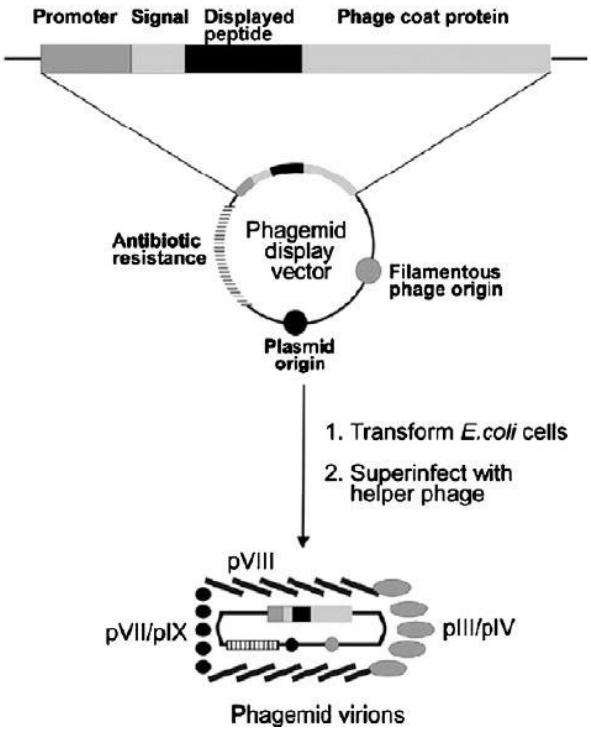

Figure 8 Steps for the construction of a phagemid particle *(Qi et al., 2012).*

To the commercial pETDuet-1 plasmid, the signal peptide pelB was added to facilitate the translocation through the bacterial membrane of phage proteins and their assembly in phage particles. Other interesting feature is the T7 promoter that is present in the commercial plasmid. This promoter allows gene transcription that affects the expression level of fusion genes. In addition, the gene responsible for the codification of the phage coat protein P3, was also added to the commercial plasmid genome (Figure 9).

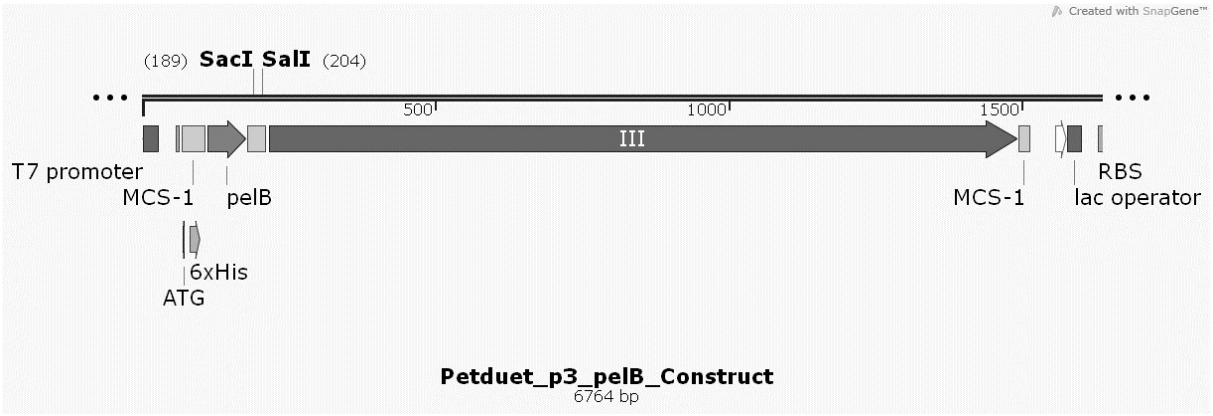

Figure 9 Modification of a commercial plasmid with the pelB signal peptide and the gene that encodes the M13 P3 protein.

In this technique, the Aβ sequences were cloned immediately before the gene 3 of the pETDuet-1 plasmid by cutting the sequences and the plasmid with the restriction enzymes SalI (NewEngland BioLabs® Inc., R0138S) and SacI (NewEngland BioLabs® Inc., R0156S), and then performing a ligation protocol. Later the gene 3 of the plasmid was merged with the helper phage gene 3 by an infection protocol, allowing the display of the Aβ sequence in the phage coat protein P3.

The Aβ sequences were obtained as in the second approach method (see section 2.5.2) but the restrictions sites KnpI and EagI were swapped for the restrictions sites SacI and SalI, respectively. Later, both sequences and the modified pETDuet-1 plasmid were double digested with SacI and SalI (Table 14).

Table 14 Reaction conditions for the digestion of plasmid and inserts.

	Plasmid	**Inserts**
DNA	500 ng	200 ng
SacI	1 µl	
SalI	1 µl	
10x NEBuffer 1.1	2 µl	
Nuclease free water	Up to 20 µl	

The digestions were incubated at 37 °C for 5 hours. Afterwards the enzymes were inactivated at 65 °C for 20 minutes. After digestion a ligation was performed using T4 DNA ligase and the used conditions were the same described in section 2.2.2.

The ligation was incubated overnight at 16 °C. After incubation, T4 DNA ligase was inactivated at 65 °C for 10 minutes. Then, 5 µl of the ligation product were transformed into chemical competent cells (see section 2.3.2). To the transformed cells 900 µl of SOC medium were added and the mixture was left to grow at 37 °C and 200 rpm. Finally the cells were plated into LB agar plates with a concentration of 20 mg/ml of ampicillin (NzyTech, MB02101) and incubated at 37 °C overnight.

Using a white tip, some white colonies were picked and dipped into a PCR tube containing 20 µl of nuclease free water. The same tip was also then streaked into a fresh agar

plate with a final concentration of 20 mg/ml of ampicillin. All the colonies were plated in the same plate. The plates were incubated overnight at 37 °C and then stored at 4 °C.

A colony PCR reaction was performed using 5 µl of the master mix, represented in the Table 15.

Table 15 Colony PCR protocol.

Component	*Per* tube
5X KAPA Taq Buffer	2.5 µl
10 mM KAPA dNTP Mix	0.5 µl
10 µ M Forward Primer	1 µl
10 µ M Reverse Primer	1 µl
5 U/µl KAPA Taq DNA Polymerase4	0.1 µl

The primers sequences and the PCR protocol are present in Table 16 and 17, respectively.

Table 16 Used primers to confirm the insertion of Aβ sequences into the plasmid.

Primer	5'- 3' Sequence
Forward (# pETDuet_1)	5' ATCGATCTCGATCCCGCGAA '3
Reverse (# 92)	5' CTAGTTATTGCTCAGCGGT '3

Table 17 PCR reaction.

Step	Temperature	Time	Cycles
Initial Denaturation	95	30s	1
Denaturation	95	10s	25-30
Annealing	48	30s	
Extension	72	30s	
Final Extension	72	30s	1
Hold	4	Hold	Hold

After the PCR reaction, the correct length of the insertion of the peptide of interest was confirmed by loading 4 µl of the PCR product in a 2 % agarose gel. The positive clones were sent to sequencing for correct sequence confirmation (see section 2.4.2), using the # pETDuet_1 primer.

a. *Infection with helper phage M13KO7*

An inoculum of 50 ml LB medium with a final concentration of 20 mg/ml of ampicillin and 100 µl of an overnight colony culture was made. The inoculum was left to grow at 37 °C and 250 rpm until a slight turbidity could be seen (with an OD_{600}<0.05). After incubation, 50 µl of the M13KO7 helper phage (1 x 10^8 PFUs/ml) were added and the incubation carried on for 60-90 minutes. Afterwards kanamycin (NzyTech, MB02001) was added to a final concentration of 70 µg/ml, and the solution incubated overnight (14-18 hours) at 37 °C and 250 rpm.

To pellet the culture a centrifugation at 6000 rpm for 10 minutes was performed and the supernatant was transferred to a new tube. Another centrifugation was performed and 90 % of supernatant was transferred into a new tube. In order to precipitate the phage, 0.2 volumes of PEG/NaCl solution were added to supernatant and then the solution was mixed several times and left to incubate at 4 °C for 60 minutes.

The phage was recovered by pelleting down the solution at 13000 rpm for 10 minutes. Carefully, the supernatant was decanted, the pellet was resuspended in 1.6 ml TBS and divided into two 1.5 ml tubes.

Subsequently, 160 µl of the PEG/NaCl solution were added to each tube and after resting for 5 minutes at room temperature, the mixture was centrifuged 10 minutes at high speed (17 000 rpm). After decanting the supernatant each phage pellet was resuspended in 300 µl TE. DNA extraction was performed following the protocol with phenol/chloroform (50/50: v/v; twice) and chloroform. Later, 30 µl of 2.5 M sodium acetate (Panreac) pH 4.8, and 2-2.5 volumes of ethanol 100 % were added for DNA precipitation at -20 °C for ≈ 2 hours. The DNA was pelleted, the supernatant discarded and allowed to dry at 37 °C for 30 minutes. Finally, the dried pellets were resuspended in 30 µl of TE buffer.

To check if the Aβ sequences were present in the phagemid genome, the samples were sequenced using the primer forward #237 that amplified the region of interest of the gene 3 (see section 2.4.2).

2.6 Immunohistochemistry assays

Immunohistochemistry (IHC) combines anatomical, immunological and biochemical techniques to identify discrete tissue components by the interaction of target antigens with specific antibodies tagged with a visible label. IHC makes it possible to visualize the distribution and localization of specific cellular components within cells and in the proper tissue context.

2.6.1 Single staining

Slides containing 10 µm cryosections from the hippocampus of a wild type mice (control) and of a transgenic mice APPswe/PS1dE9 (AD-model), both with 6 month old, were used. The slides were gently provided by Dr Helmut Kessels from the Netherlands Institute for Neuroscience.

The slides were rinsed in tap water until antigen retrieval could be performed. This step avoids drying of the slides and consequently non-specific antibody binding with therefore high background staining.

To maximize antibody binding, antigen retrieval was performed by heating slides in 10 mM sodium citrate buffer pH 6.0 (Sigma, W302600) in a microwave (700 W) 3 times for 5 minutes. Then the slides were left to rest at room temperature for about 20 minutes. After

cooling, the slides were washed in TBS buffer with 0.1 % of Tween 20 (OmniPur, Merck) (TBST), 2 times for 5 minutes.

Later, tissue samples were blocked using 5 % bovine serum albumin (BSA, NzyTech) in TBST solution added directly onto the specimen and incubated at room temperature for 30 minutes. Again the slides were washed in TBST, 2 times for 5 minutes.

Next, 100 µl of the phage ($1x10^{10}$ PFUs/ml) were added to the tissue for an overnight incubation at 4 ºC. At the same time an incubation with the wild type phage was performed.

On the next day the slides were washed in TBST two times for 5 minutes and subsequently 100 µl of primary rabbit anti-fd bacteriophage antibody (Sigma, B7786) (working dilution of 1:1000 in BSA 1 %) were added to the slides and incubated at 4 °C overnight.

After incubation the slides were washed in TBST 2 times for 5 minutes and then a FITC-labeled goat anti-rabbit IgG secondary antibody (Sigma, F9887) (working dilution of 1:40 in BSA 1 %) was incubated 2 hours at room temperature. Finally the slides were washed 2 times for 5 minutes with TBST and then mounted with Vectashield.

The results were analyzed using an Epifluorescence microscope (Olympus BX51) coupled with a DP71 digital camera and three sets of filters (DAPI – 360-370/420; FITC – 470-490/520; and TRITC – 530-550/590) (OlympusPortugal SA). All images were acquired using the Olympus CellSens software.

2.6.2 Double staining

The double staining IHC was performed in an attempt to assess if the phage particle only recognizes the Aβ oligomers and not Aβ plaques.

Apart from the specific anti-M13 antibody, the commercial 6E10 antibody (BioLegend®, 803001), staining from APP to Aβ plaques, was used.

The used protocol was the same described in section 2.6.1 with a few changes. To the 1 % BSA solution in TBST, not only the anti-M13 primary antibody was added, but also the 6E10 antibody with a dilution of 1:7500. To the solution containing the secondary antibody labeled with FITC, a secondary antibody Donkey anti-Mouse IgG (H+L) labeled with Alexa Fluor® 594 (Thermo Scientific, A-21203) with affinity to 6E10, was added, diluted 1:1400. Both 6E10 and Donkey anti-Mouse IgG (H+L) labeled with Alexa Fluor® 594 antibodies were gently provided by Dr Helmut Kessels from the Netherlands Institute for Neuroscience.

2.7 M13KE Chemical Functionalization

For the modified phage particle to be traceable, the coat protein P8 was functionalized with the fluorescent dye Alexa Fluor® 488 (Thermo Scientific). Alexa Fluor® dyes are reactive molecules that can be used to add a fluorescent label to the primary amines ($R\text{-}NH_2$) of proteins. This molecule produces a conjugate with excitation/emission of 495/515 nm that is spectrally similar to fluorescein (FITC) and Cy2 conjugates.

Instead of using the common chemical conjugation with succinimidyl ester (SE) or N-Hydroxysuccinimide (NHS) ester, this method uses tetrafluorophenyl (TFP) ester instead. The functionalization with TFP esters is less susceptible to spontaneous hydrolysis during conjugation reactions than conjugation with NHS ester.

In order to obtain fluorescent phages particles, a solution mixing the Alexa dye and the modified phages was added to a sanitized Microsep Advance Centrifuge Device 10 K MWCO (Pall Corporation), so that the phage molecules could be separated from the free dye. Conjugated solutions were added to the tube reservoir where phages (conjugated and non-conjugated) would remain, while the other components, such as free fluorescent molecules, will pass through the membrane to the filtrate receiver. Before sample filtration columns had to be prepared.

a. *Column preparation*

Before use, the columns were sanitized as following described. For the wash protocol, 3 ml of cold ethanol 70 % were added into the column and a centrifugation at 7500 rpm, 4 °C during 5 minutes was carried out. Next, the volume was discarded and the columns were washed twice with 1 ml of phosphate-buffered saline (PBS) pH 7.4 (137 mM NaCl, 2.7 mM potassium chloride (KCl), 10 mM sodium phosphate dibasic and 2 mM potassium dihydrogen phosphate, all from Panreac) at the same conditions. Since the membranes should not be dried, the sanitization procedure was conducted immediately before adding the conjugation solution.

b. *Sample preparation*

To a solution of 1 ml of the mutant phage particle ($1x10^{10}$ PFUs/ml), 0.2 volume of PEG/NaCl solution were added for phage precipitation. The solution was left to incubate at 4 °C for 60 minutes. To pellet the phage, a centrifugation at 10000 rpm for 10 minutes was

performed. Phage pellet was then resuspended in 150 µl of 0.1 M sodium bicarbonate buffer pH 8.3 (Sigma).

Immediately before use, the amine-reactive dye was dissolved in dimethylsulfoxide [(DMSO), Sigma-Aldrich Co. LLC] at a final concentration of 1 mg/ml.

While stirring the phage solution, 15 µl of the reactive dye solution were added. The reaction was incubated for 1-2 hours at room temperature with continuous stirring.

After incubation, the solution was loaded into the washed columns and a centrifugation at 7500 rpm, 4 °C during 5 minutes was carried out. To remove the conjugated particles that were still in the column, 1 ml of PBS was loaded and a centrifugation performed. The resultant solution was stored at 4 °C until usage.

3. RESULTS AND DISCUSSION

3.1 M13KE Quantification

After being produced and stocked, M13KE phage was quantified by PFUs in a LB/IPTG/X-Gal plate. Successive dilutions were made and the 10^{-8} dilution was chosen since the plates presented between 10 and 100 plaques (Figure 10). Plaques were counted and PFUs were calculated accordingly with equation 1. Since 23 plaques were counted at 10^{-8} dilution in a 10 µl drop, the concentration of M13KE phage was found to be 2.3×10^{11} PFUs/ml.

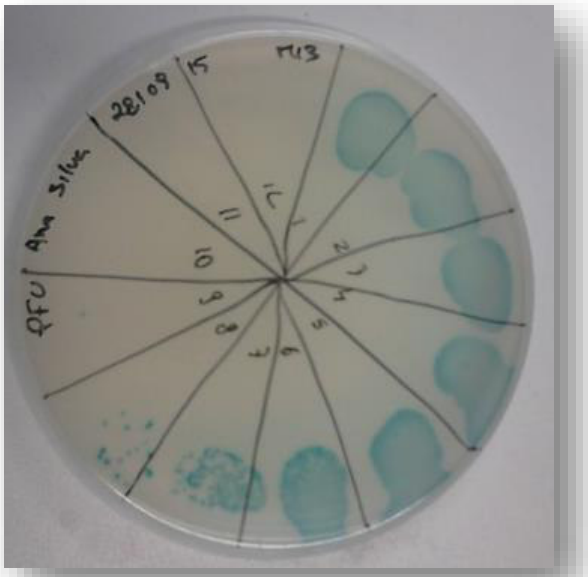

Figure 10 Plate of M13KE quantification with 12 drops of successive dilutions of the phage solution.

In order to manipulate the M13 phage to clone the inserts of interest it was necessary to extract its dsDNA. The DNA concentration was measured in NanoDrop1000 Spectrophotometer (Table 19).

Table 18 M13 phage dsDNA quantification.

Sample	[DNA] ng/µl	Ratio A260/280	Ratio A260/230
M13	242,5	1,76	1,26

The A260/280 ratio is generally used to determine protein contamination of a nucleic acid sample. For pure DNA, A260/280 ratios should be around 1.8. A lower ratio indicates the presence of proteins, phenol or other contaminants that absorb strongly at or near 280 nm. High 260/280 purity ratios may suggest sample contamination with RNA, showing problems in the extraction protocol. The A260/230 ratio indicates the presence of organic contaminants, such as phenol, carbohydrates, chaotropic salts and other aromatic compounds. Samples with 260/230 ratios below 1.8 are considered to have a significant amount of these contaminants. In a pure sample, the A260/230 should be close to 2.0. A high A260/A230 ratio may be the result of performing a blank measurement on a dirty pedestal or using an inappropriate solution for the blank measurement (Kilby, 1976; Wilfinger et al., 1997).

In this case, the A260/280 ratio has the indicated value, but the A260/230 ratio suggests the presence of contaminants. This value indicates that the sample may have not been fully cleaned, resulting in a contamination with salts, metabolites or soluble macromolecular cellular components. To ensure that the DNA was contaminants free, an extra cleaning step was performed to the protocol in the following purifications, leaving only the DNA of interest on the separating membrane.

3.2 Inserts synthesis

To obtain both inserts Aβ 30-39 (AIIGLMVGGV) and Aβ 33-42 (GLMVGGVVIA), two different techniques were applied: (i) One based on the synthesis of libraries for phage display described on the New England Biolabs Phage Display Manual, but instead of using a random library we used the peptide sequences already described, with affinity to the Aβ oligomers and (ii) and another based in a 100 % complementarity method to anneal two primers.

For a better understanding of the obtained results, the SnapGene software was used to perform an *in silico* cloning of the inserts into the M13 genome (Figure 11). Using this system

it was also allowed the visualization of what should be the expected size of the inserts obtained by PCR reaction.

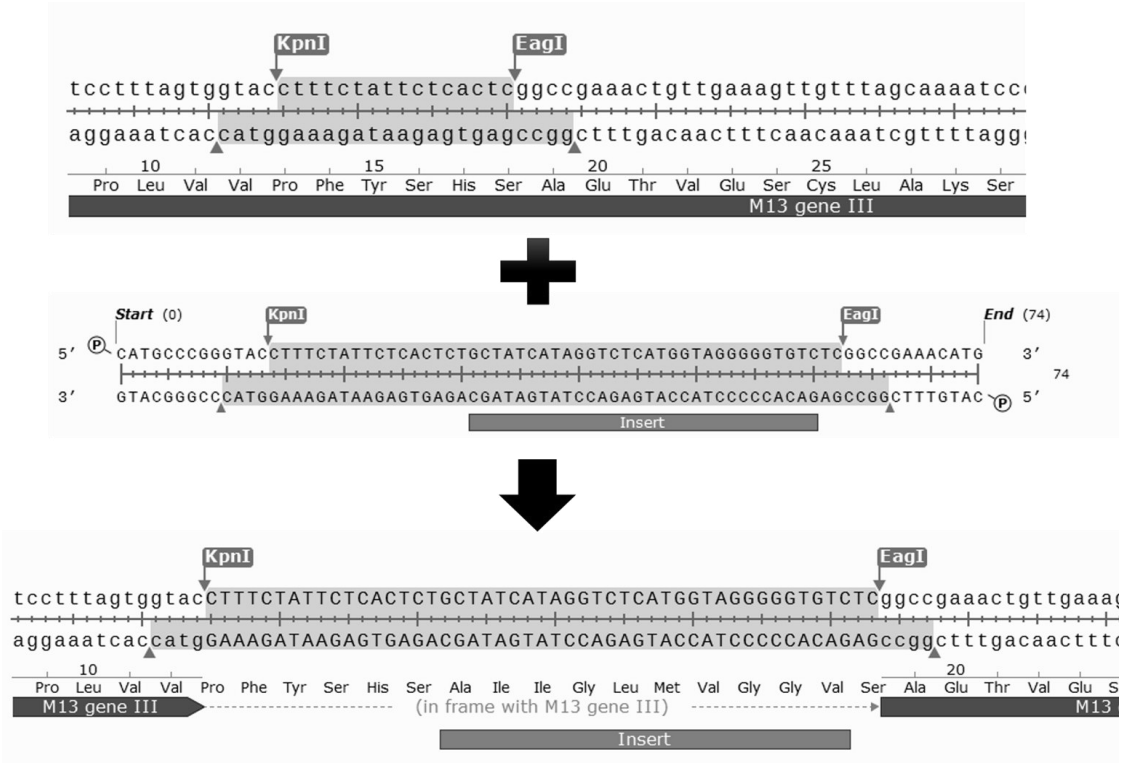

Figure 11 Schematic representation of the digestion:ligation protocol of one of the Aβ inserts, with the vector M13.

To verify if the insert synthesis was successful, the resulting PCR product visualized on a 2.5 % agarose gel (Figure 12).

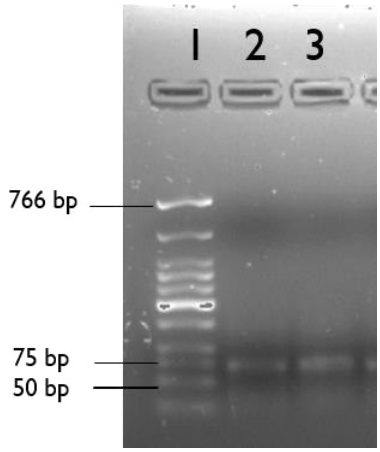

Figure 12 Inserts size confirmation of the first technique. *1- Low Molecular Weight ladder; 2 - Insert Aβ 30-39; 3 - Insert Aβ 33-42.*

Taking into consideration the designed primers size and the *in silico* results (Figure 11) a band with 74 bp size should appear. Observing the gel, it is accurate to assume that the inserts have the correct size by comparison with the low molecular weight (LMW) ladder. Once the ligation vector::insert was confirmed, the DNA was purified and the concentration measured (Table 19).

Table 19 DNA quantification of the inserts.

Sample	[DNA] ng/µl	Ratio A260/280	Ratio A260/230
Aβ 30-39	63.9	1.83	3.23
Aβ 33-42	37.2	1.60	3.03

Analyzing the purity of the DNA samples, the DNA from the Aβ 30-39 sequence shows the correct level of purity in the A260/280 ratio, but the A260/230 suggests that the blank solution could be contaminated. The DNA from the Aβ 33-42 show the same problems in the A260/230 ratio value, but doesn't have the same level of purity. To safeguard a better level of purity, the extraction protocol was slightly changed, increasing the duration of the drying pellet step. Thereby the residues of phenol and ethanol were reduced, improving the purification ratios.

As in the first technique, before proceeding to the cloning protocol, the ligation of the inserts obtained in the second approach with the M13 vector was tested *in silico*. Both the size of the insert as it ligation with the M13 vector are represented in Figure 13.

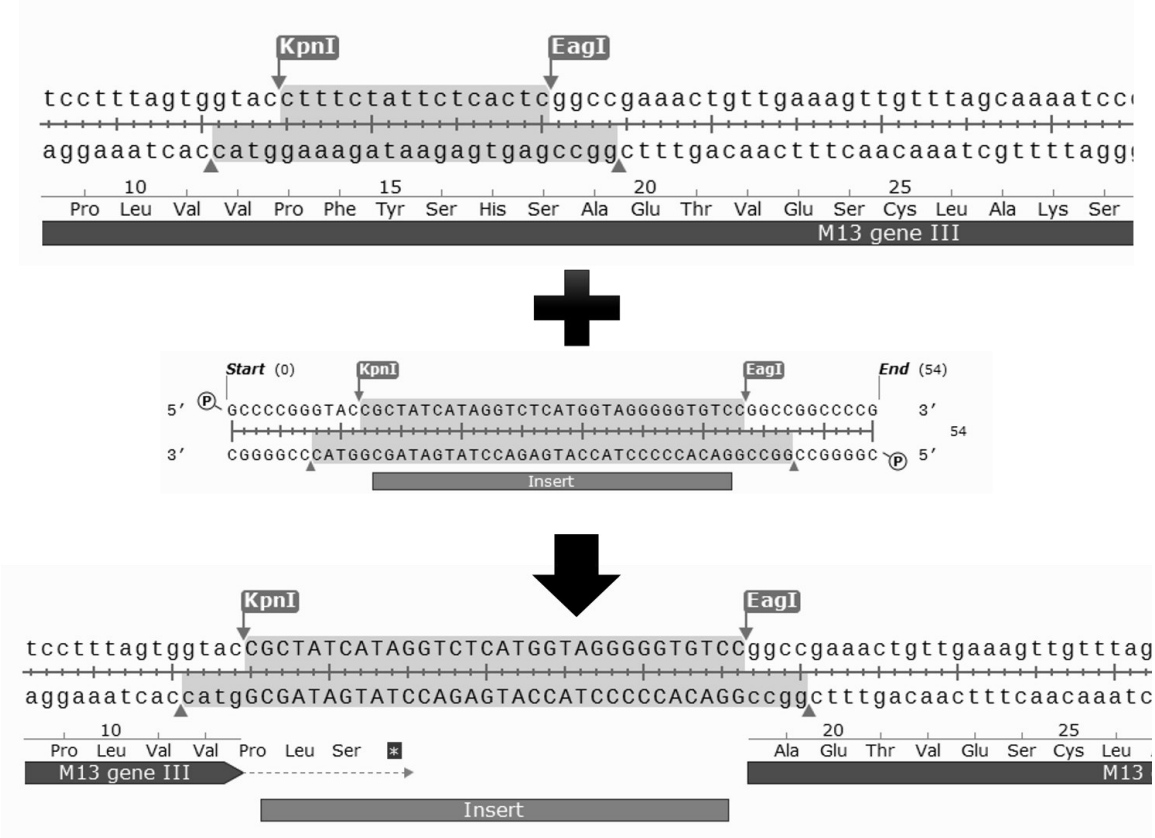

Figure 13 Schematic representation of the digestion: ligation protocol of one of the Aβ inserts, with the vector M13.

To verify if the insert synthesis was successful, the resulting PCR product was visualized on a 3 % agarose gel (Figure 14).

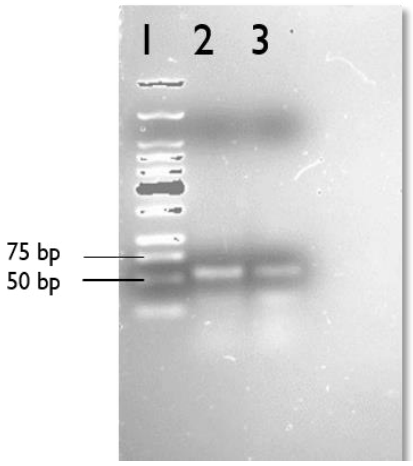

Figure 14 Inserts size confirmation of the second technique. *1- Low Molecular Weight ladder; 2 - Insert Aβ 30-39; 3 - Insert Aβ 33-42.*

Once again, the results were as expected. Figure 14 shows an expected size of the insert of 54 bp. By comparison with the 50 bp band of the LMW (lane 1), we can observe that both inserts have the expected size. After size confirmation the DNA concentration was measured (Table 20).

Table 20 DNA quantification of the inserts.

Sample	[DNA] ng/µl	Ratio A260/280	Ratio A260/230
Aβ 30-39	102,5	1,75	1,38
Aβ 33-42	75,3	1,73	1,40

In both samples the level of purity is acceptable by evaluation of the A260/280 ratio, but the A260/230 ratio may indicate the presence of organic contaminants like phenols or salts. Since the base solution (Tris-HCl pH 8.0) used to make the annealing of primers has salts on it constitution, it is possible that this factor had influenced the purity ratio. Therefore, in order to increase the purity level of the samples, the blank solution was remade with ultrapure water and them autoclaved, assuring a minimum of contaminants.

Although very similar, this approach was used to replace the first one due to unnecessary purification of the inserts, leading to less DNA loss, less time consuming.

3.3 M13KE Genetic Manipulation

3.3.1 Transformation Process

Prior to the transformation protocol, the M13KE dsDNA, obtained in section 2.1.4, was digested as well as the inserts of interest. The inserts from both techniques were digested in the conditions described in sections 2.5.1 and 2.5.2. After double digestion of the inserts and the M13KE DNA, a ligation protocol was performed between the M13 vector and the encoding fragments of each insert. After the electroporation process (see section 2.3.1) with the manipulated DNA, 3 plates with different volumes of transformed cells were plated: 10 µl, 100 µl and the remaining pelleted cells. In most cases the plate with 10 µl did not show any colonies (Figure 15).

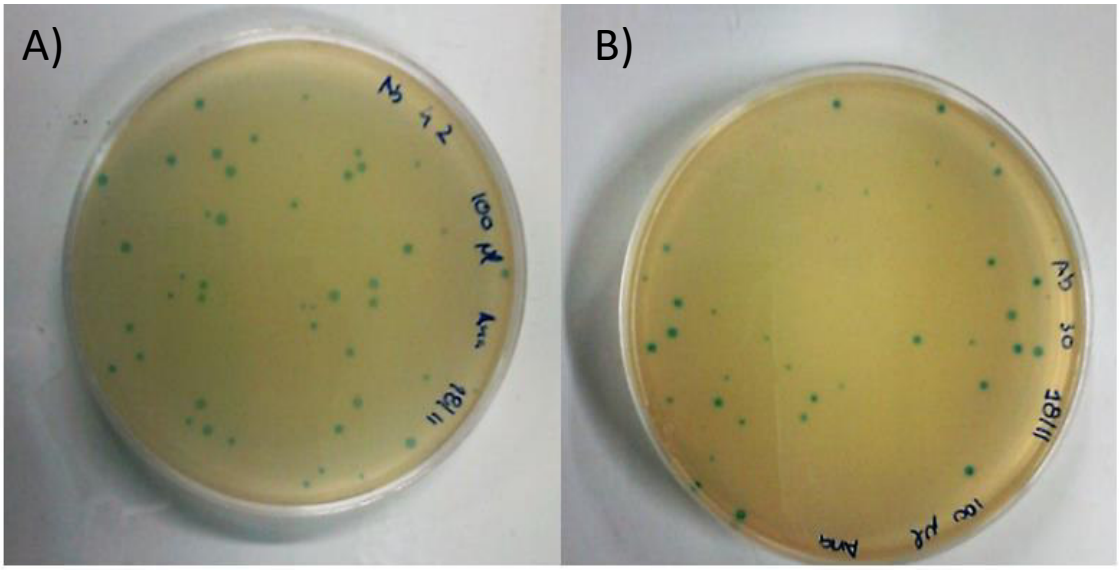

Figure 15 JM109 electrocompetent cells transformed with A) M13::Aβ 33-42 and B) M13::Aβ 30-39. *The ligations were performed using the inserts obtained with the second technique.*

After a successful transformation, some random clones were picked and their DNA extracted and quantified (Table 21) in a NanoDrop1000 Spectrophotometer.

Table 21 DNA quantification of selected clones from transformation process.

Sequence	Clone	[DNA] ng/µl	Ratio 260/280	Ratio 260/230
Aβ 30-39	1	45.8	3,22	-------
	2	22,8	2,68	-------
	3	58,6	6,14	-------
	4	51,6	2,39	-------
	5	11,2	6,80	-------
Aβ 33-42	1	9,20	3,15	-------
	2	89,7	2,01	-------
	3	62,3	10,22	-------
	4	29,5	15,36	-------
	5	77,5	3,82	-------

The used extraction protocol makes the DNA samples quite impure, mostly because of the use of components like phenols. Even with successive washes with ethanol the contaminants remained in the sample. Other reason for the impurity of the sample may be residual ethanol that may have not been well dried. In order to overcome the bad purification ratios, the new DNA extractions were done using the purification kit referred to in section 2.1.4. This modification allowed cleaner samples and less complications were observed in the DNA amplification by PCR.

3.3.2 M13KE::Inserts Ligation – Confirmation by PCR

Using the extracted DNA, an amplification of the zone of gene 3 was made in order to identify the positive clones (with the peptide insertion). To that end, PCR amplification was performed using specific primers that amplify the gene 3 fragment. PCR amplified fragments were analyzed in a 2.5 % agarose gel (Figure 16). The positive PCR fragments should be above the 350 bp lane.

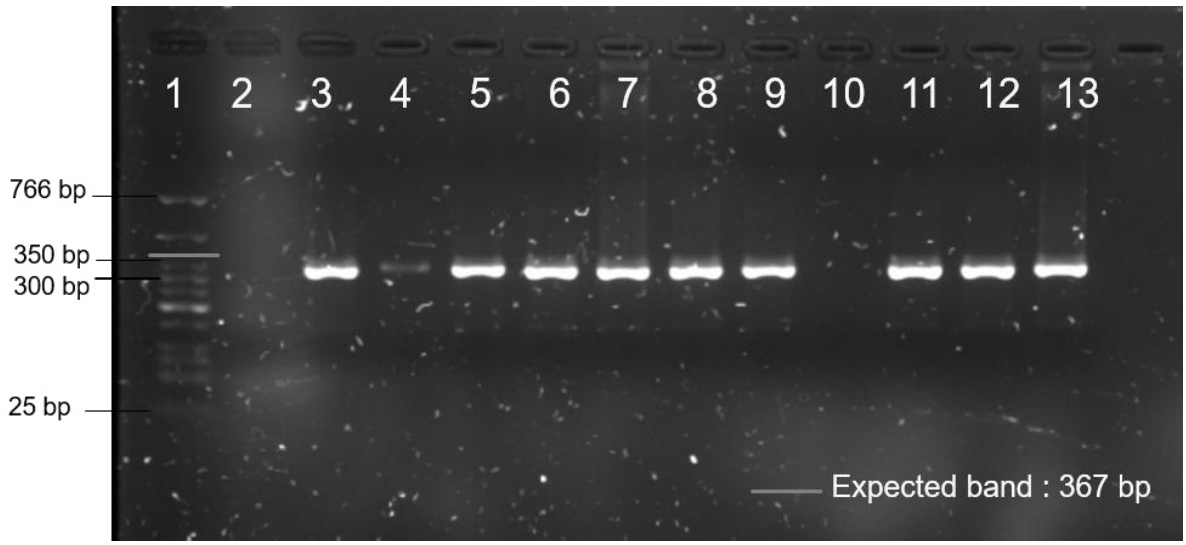

Figure 16 Amplification of the gene 3 sequence containing the ligation of M13KE with the interest inserts obtained from the second technique*. 1 - Low Molecular Weight; 2-6 - Aβ 30-39 clones; 8-12 - Aβ 33-42 clones; 7 and 13- M13 wild type.*

Comparing the lanes 2-6 (Aβ 30-39 clones) and the 8-12 lanes (Aβ 33-42 clones) with lanes 7 and 8 (wild type phage), no differences were observed, and all bands have the same size. This result shows that the insert has not been cloned into the vector.

The ligation protocol between the inserts of both techniques and the vector was performed multiple times. Other conditions were also tried, such as the optimization of digestion and ligation times or DNA and enzyme concentrations but not only once the correct peptide sequence was present in the M13 genome.

In some of the attempts, differences between the clones and the controls were observed but the inserted DNA sequence never corresponded to the sequence of interest. Other clones were also sequenced, but the results came negative (Figure 17).

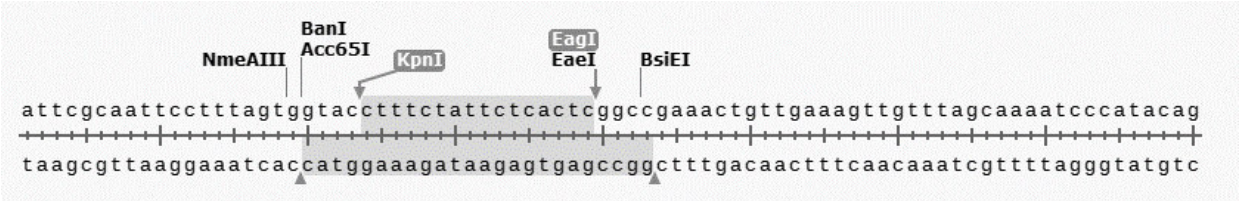

Figure 17 Example of a negative sequencing result. *There is no presence of the Aβ sequence between the KpnI and EagI restriction sites. The results were analyzed using the program SnapGene™.*

There are a few possibilities to explain the non-insertion of the inserts. The ligation may have not occurred because small amounts (ng) of oligonucleotides inserts represent a large molar excess when compared to the vector amount, due to the small size of the insert compared to the vector. Even following a molar ratio of 3:1 (insert:vector) a ligation cannot be assured. Also, T4 DNA ligase efficiency may not have been enough precluding the ligation. Alternatively, the fact that clones without insert are more abundant than positive clones, because it is more usual for the phage to incorporate the wild type protein rather than the modified version, it is possible that only negative clones were selected (Ghosh et al., 2012a). But the most likely reason was the ability of the M13KE to modify its own genome to reach a more stable state. Taking into account that the P3 protein is responsible for the translocation of the viral DNA into the host cytoplasm during infection of Gram-negative bacteria, it is possible that the ligation occurred, but the phage ends up expelling the insert sequence during the phage replication process (Qi et al., 2012).

3.3.3 Round PCR

To overcome the limitation found in the previous approaches of cloning, a different approach was used. In the round PCR the gene 3 of the M13 genome was modified by a PCR protocol, ensuring that the amplified DNA contains the Aβ inserts sequences immediately after the restriction enzyme site of KpnI (Figure 18).

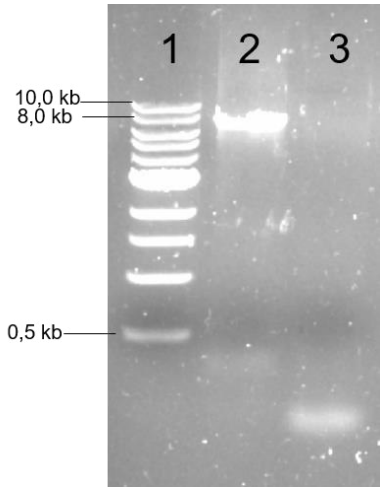

Figure 18 Amplification of the modified M13KE DNA with the Aβ insert. *The samples were loaded in a 1 % agarose gel. 1 – 1 Kb ladder; 2 – Round PCR sequence Aβ 30-39; 1 – 32 – Round PCR sequence Aβ 33-42.*

Figure 18 represents the result of the PCR product which gave rise to the amplification of the modified DNA. The mutant M13KE genome should comprise a size of 7250 bp. It can be observed that only one of the sequences was obtained, the Aβ 30-39 (lane 2). Comparing the sequence band with the 8 kb band of the DNA ladder it can be assumed that the PCR product has the correct size. After confirmation, the PCR product was cleaned using the NucleoSpin® Gel and PCR Clean-up Kit.

For transformation processes, the obtained M13 vector with the Aβ 30-39 sequence had to be circularized, a step that increases the transformation efficiency (ADAM, GONZA´LEZ-BLASCO, RUBIO-TEXEIRA, & POLAINA, 1999). If the vector stays linear, it is likely that no colonies appear. For that, T4 DNA ligase was used and then the circular DNA was transformed into chemical competent cells.

After transformation, random blue colonies were picked and their DNA extracted. Once again, an amplification of the gene 3 was performed (Figure 19). The conditions used were the same as in section 2.4.

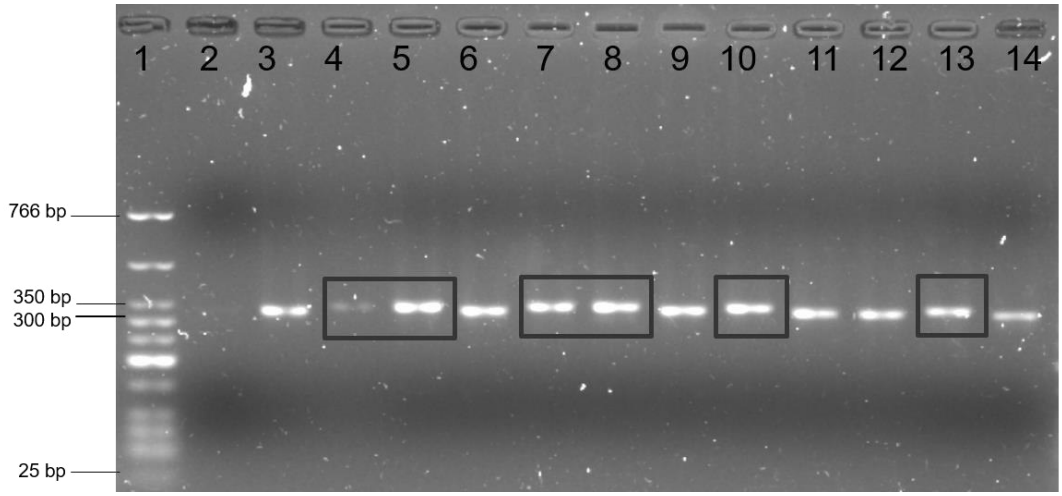

Figure 19 Amplification of the gene 3 zone containing the Aß sequence. *Samples were loaded on 2.5 % agarose gel. 1 - LMW; 2 and 14- M13 wild type; 3-13 - Aß 30-39 clones. Black squares shown the clones with different sizes comparing to the wild type phage.*

Figure 19 shows the amplification results of eleven randomly picked clones. Significant differences between some clones and the wild type phage can be observed. The clones from lanes 4, 5, 7, 8, 10 and 13 are above the 350 bp band from the LMW band (lane 1) and also above the band from the wild type phage (lanes 2 and 14). The PCR product of these clones was purified and sent to sequence (see section 2.4.2) (Table 22).

Table 22 Sequencing results of Aß 30-39 clones from Round PCR. *In red the restriction site of KpnI enzyme, in green the restriction site of EagI enzyme and in purple, the sequence of the peptide of interest. The bold letter represent the codon that translate the first amino acid, and the underline letter show the mutation occurred in the first amino acid.*

Clone	Nucleotide Sequence	Peptide Sequence
2	GGTACCTTTCTATTCTCAC**GT**AGGGGGTGTATCGGCCG	VGGV
3	GGTACCTTTCTATTCTCAC**GG**AGGGGGTGTATCGGCCG	GGGV
5	GGTACCTTTCTATTCTCAC**GG**AGGGGGTGTATCGGCCG	GGGV
6	GGTACCTTTCTATTCTCAC**GG**AGGGGGTGTATCGGCCG	GGGV
8	GGTACCTTTCTATTCTCAC**GG**AGGGGGTGTATCGGCCG	GGGV
11	GGTACCTTTCTATTCTCAC**GG**AGGGGGTGTATCGGCCG	GGGV

For clone 2, part of the correct sequence was inserted into the M13 phage genome. In the other five clones a mutation occurs in the first inserted amino acid, changing a Valine (V) for a Glycine (G). Once again these results show how the M13 phage has the capacity to expel unfamiliar DNA sequences and stabilize its expression. Peptides are displayed in the coat protein P3, which modulates infectivity by binding to the F-pilus of the host cell. As a result, there is a biological selection against certain displayed sequences during *in vivo* amplification, particularly sequences with multiple positive charges and unpaired cysteines (Fukunaga & Taki, 2012; Schmiedl et al., 2000). Taking into account these results, it is possible that the M13 phage rejected the Aβ inserts due to its amino acid composition.

Even if a full insertion of the peptide of interest was not obtained, the work was continued with the four amino acid mutant by taking into consideration the work done by Lionel Larbanoix and his co-workers (Larbanoix et al., 2011). In their work, an Aβ 42 library of six amino acids was displayed in the P3 protein. None of the displayed peptides obtained the exact sequence or the full sequence. From a 5 amino acid sequence, IHC assays on brain sections harvested from a mouse model of AD were performed, in order to study the phage particle affinity to the Aβ protein.

With our modified phage, IHC assays were performed, to evaluate if our particle also had affinity towards the Aβ oligomers.

3.3.4 Phagemid cloning system

The use of the phagemid approach comes to overcome the instability of the M13KE phage. This method arises to create a particle capable to express the entire Aβ peptide. For the construction of phagemid, the pETDuet-1 plasmid was used. The final purpose of this approach was to merge the plasmid with a helper phage. In the plasmid preparation, a signal peptide, the pelB which simplifies the translocation of phage proteins, and the gene that encodes the P3 protein, were added to the commercial pETDuet-1 plasmid. Instead of inserting the peptide in the phage genome, the insert was placed before the gene 3 of the modified pETDuet-1 plasmid. Phagemids are very stable as cloning vector (Rajaram & Vermeeren, 2014), allowing the insertion of the entire peptide sequence. After confirmation of the plasmid modification with the Aβ sequence, its DNA was fused to the DNA of the helper phage M13KO7, which provides all the proteins necessary to generate a new phage (see section 2.5.3). Unlike conventional

plasmid vectors, phagemids contain elements that cause them to be packaged into phage capsids as ssDNA (Lund et al., 2010).

After being digested, the two Aβ sequences and the modified pETDuet-1 plasmid were ligated using the T4 DNA ligase enzyme. Using the primers described in section 2.4 the gene 3 fragment of pETDuet-1 plasmid was amplified by PCR (Figure 20).

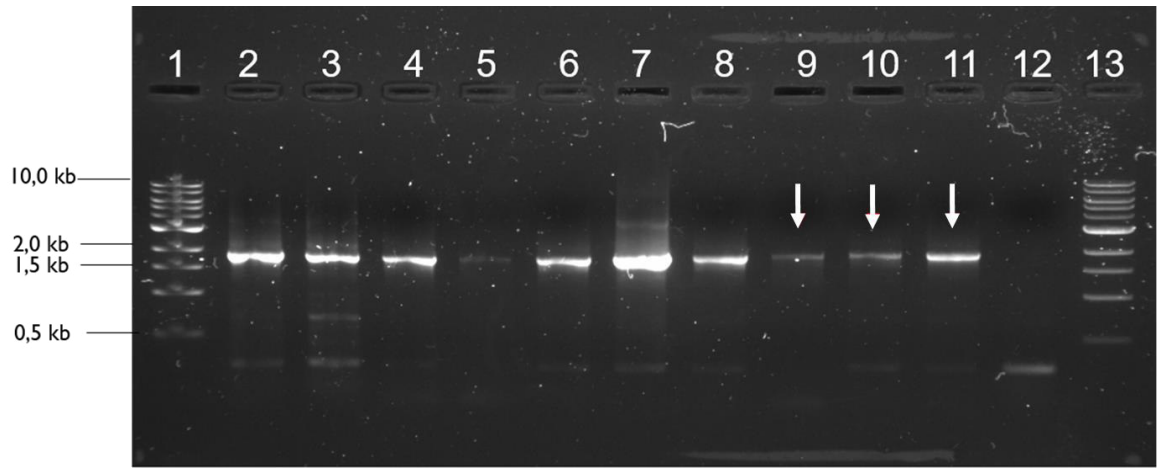

Figure 20 Amplification of the gene 3 zone from pETDuet-1, containing the Aβ sequence. *Samples were loaded on a 1 % agarose gel. 1 and 13– 1 kb DNA ladder; 2-6 - Aβ 33-42 clones; 7- Negative control (plasmid without insert); 8-12 - Aβ 33-42 clones. Red arrows show the clones with different sizes comparing to the negative control band.*

Considering the electrophoresis results, we can observe that the amplification appears in the expected size, since the plasmid without the insert should have 1849 bp (lane 7). Comparing lanes 9, 10 and 11 with lane 7, we can see that these clones are slightly above lane 7. This result indicates that an insertion of DNA into the plasmid genome occurred. The same protocol was performed for the Aβ 30-39 sequence. The electrophoresis results can be checked in annex I. Two clones (clone 9 and 10) were picked for further analysis.

Figure 21 represents the expected location of the Aβ sequences after a successful ligation protocol.

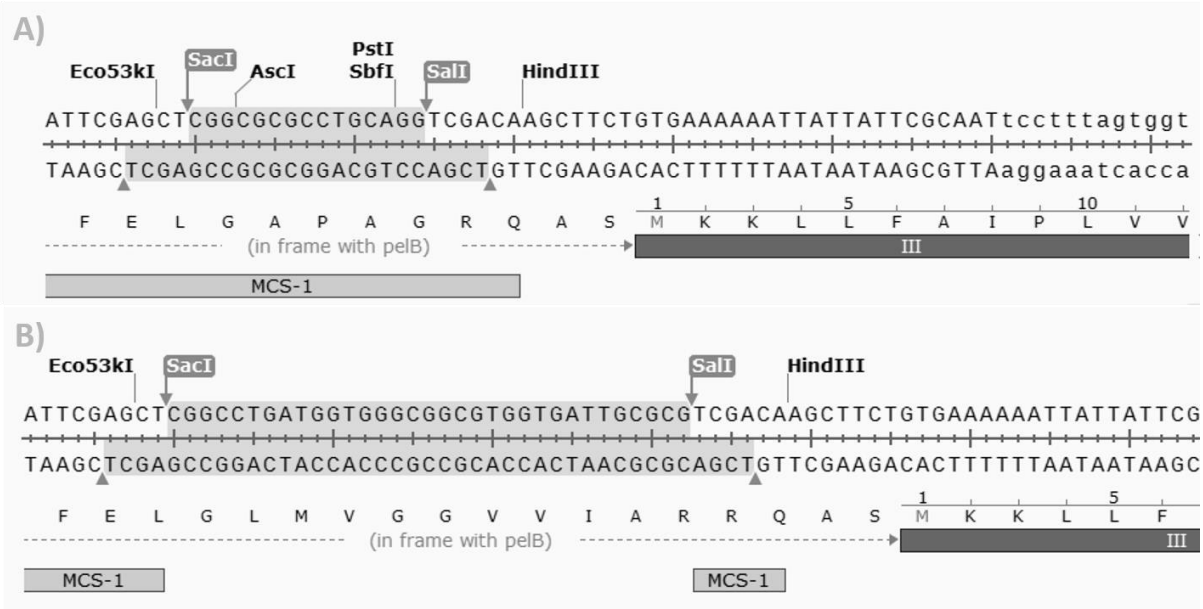

Figure 21 Cloning representation between the modified plasmid with the Aβ 33-42 sequence.

To verify if the inserted DNA sequence corresponds to the correct Aβ sequences, the clones were sent to sequence using the # pETDuet_1 primer (see section 2.5.4). In the sequencing results it should be visible the phage gene 3 zone with the insert on the right before the gene (Table 23).

Table 23 Sequencing results of Aβ 30-39 and Aβ 33-42 clones from the Phagemid approach. *In red the restriction site of SacI, in green the restriction site of SalI and in purple, the sequence of the peptide of interest.*

Clone		Nucleotide Sequence	Peptide Sequence
Aβ 30-39	9	GAGCTCGCGATTATTGGCCTGATGGTGGGCGGCGTGCGTCGAC	AIIGLMVGGV
	10	GAGCTCGCGATTATTGGCCTGATGGTGGGCGGCGTGCGTCGAC	AIIGLMVGGV
Aβ 33-42	7	GAGCTCGGCCTGATGGTGGGCGGCGTGGTGATTGCGCGTCGAC	GLMVGGVVIA
	8	GAGCTCGGCCTGATGGTGGGCGGCGTGGTGATTGCGCGTCGAC	GLMVGGVVIA
	9	GAGCTCGGCGCGCCTGCAGGTCGAC	------

Evaluating the sequencing results, it can be seen that the entire Aβ 30-39 sequence (AIIGLMVGGV) was inserted into the plasmid genome in clones 9 and 10, and the Aβ 33-42 sequence (GLMVGGVVIA) in clones 7 and 8.

Since the sequencing results were positive for some of the clones, an infection with helper phage M13KO7 was performed.

After the infection protocol with the helper phage M13KO7, the DNA of the new phage particle was extracted and purified. This DNA was sent to sequence using the primers of section 2.4.2. In the sequencing results the phage gene 3 zone should be visible with the insert right before it. Figure 22 shows the sequencing results.

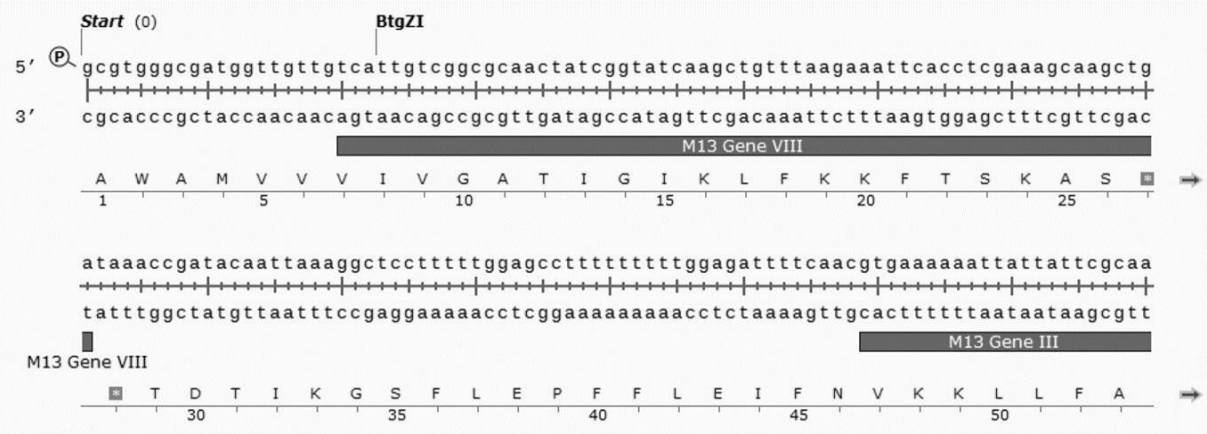

Figure 22 Sequencing results from pETDuet-1 infection with the M13KO7 helper phage.

Despite multiple attempts, the helper phage could not infect the plasmid with its DNA. As depicted in Figure 22, the results of sequencing did not show any of the sequences of interest immediately before the gene 3. This leads us to think that during the DNA infection and amplification, only the wild type helper phage DNA was amplified. Because of this, in DNA extraction, only the DNA helper phage will be found (Phipps et al., 2016).

Many drawbacks are present in the production of a functional phagemid particle. During the protocol there are many factors difficult to control, among them are the nature of the helper phage, the density of the culture at the time of infection, the multiplicity of infection of the helper phage, and the incubation time. The DNA extraction process can also influence the quality of the sample. The phenol-chloroform method cannot provide a complete lyse of phage particles and also is characterized by contamination with residual protein. Another factor which may have had an effect on the production of a positive phagemid particle was the used strain for the infection protocol. Host strains like JM109 can release their chromosomal and phagemid DNA into the medium due to cell lysis resulting in the contamination of ssDNA (Zhou et al., 2009).

Even though this system has been shown very promising in different reports, we were not able to obtain these particle. This difficulty can eventually be overcome with the use of a different strain and also with protocol optimizations.

3.4 Immunohistochemistry Assays

3.4.1 Single Staining

Immunohistochemistry (IHC) assays were performed in order to establish if and how our modified particle binds to Aβ oligomers. In this procedure, both slides containing hippocampus tissue of double transgenic mice APPswe/PS1dE9 model (Jankowsky et al., 2003), and slides containing hippocampus tissue from healthy mice (control) were used.

To obtain mice models with AD, genes responsible for production of proteins as the APP or the presenilin 1 or 2 (PS1/PS2) gene that regulates the production of γ-secretase, are frequently modified. These mutations are carried out in order to allow an abundant production of the Aβ human protein and the consequent plaque formation. These mutations can be single or double depending on which of the genes are modified. In this work APPswe/PS1dE9 double transgenic mice were used. This mice model presents a very high level of Aβ even with 6 months of age, allowing the recognition of Aβ peptide by ligation of our modified phage (Puzzo et al., 2014; Xiong et al., 2011).

To ensure the affinity of our modified phage to the Aβ oligomers, IHC assays were performed incubating the M13 wild type phage (control) and the mutant phage with the 4 amino acids of Aβ 30-39 sequence, obtained in the Round PCR approach (see section 2.5.3). This phages were tested in both healthy and AD tissues (Figure 23).

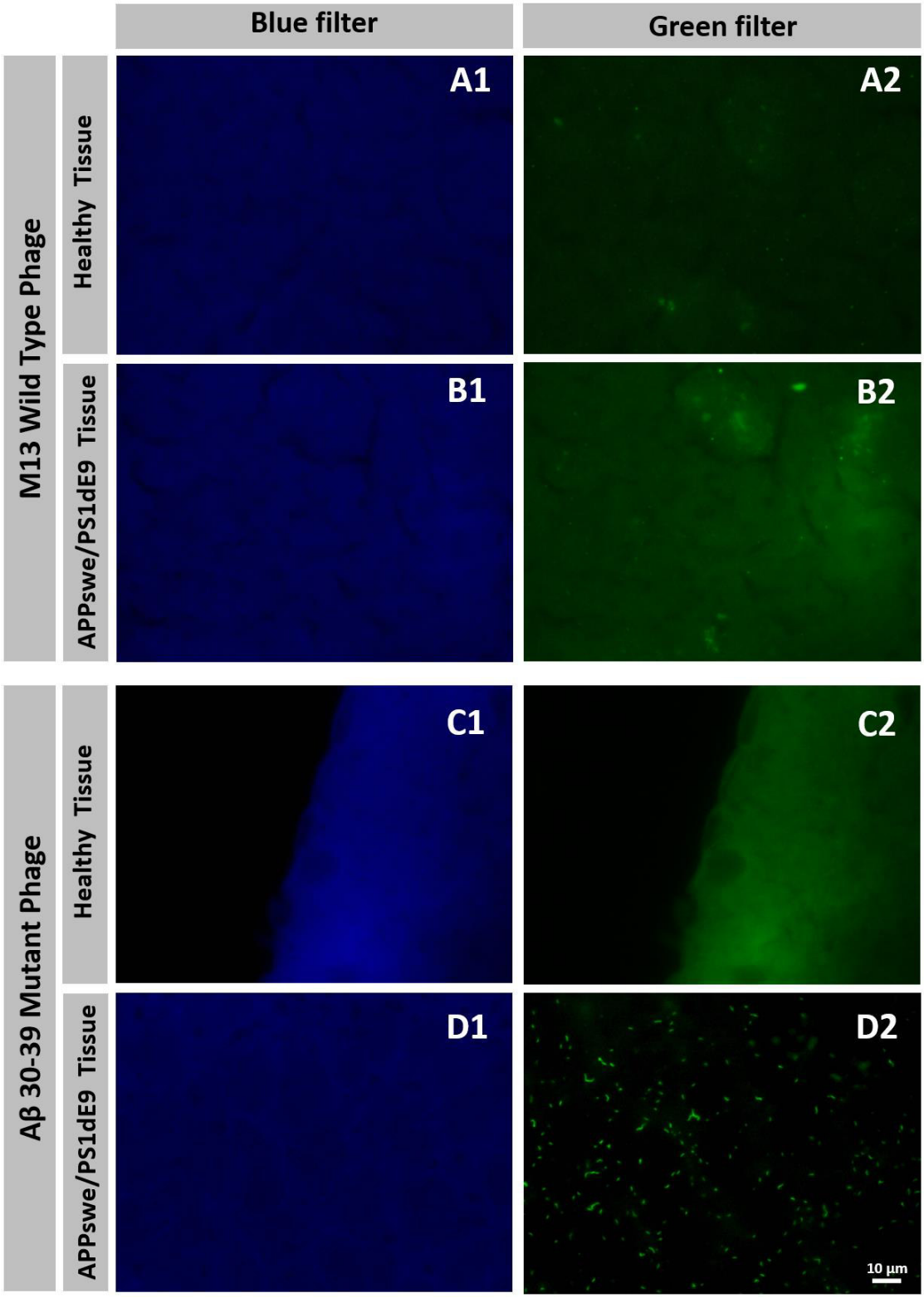

Figure 23 Epifluorescence images showing the M13 wild type and the Aβ 30-39 mutant phage particles incubated with samples of healthy tissue and AD model tissue. *Columns correspond to different microscope filters (DAPI on the left and FITC on the right). A and B correspond to the M13 wild type incubation and C and D to the Aβ 30-39 mutant phage. All images were acquired using 100 × 1.30 NA oil objective lens.*

In the incubation of the M13 wild type phage, an absolute absence of staining in both tissues would be expected, since the wild type phage particle by itself is not able to bind to the Aβ oligomers.

One of the features of filamentous phages is their lack of tropism towards animal cells. Not owning the ability to infect or link the cells or tissues, the wild type phage is incapable of connecting to the brain cells, being eliminated in the washing process (Pointer et al., 2014). The only way filamentous phages could get some affinity to mammalian cells would be expressing a recognition sequence in its surface (M. W. Smith et al., 2012). Once more, these facts reaffirm the ability of our mutant phage to bind to Aβ oligomers.

During the analysis of the tissues, sporadically some fluorescents points occurred in both types of tissues. It probably would not be the wild type phage binding to the mouse tissue, but the contaminants that were not removed in the wash steps, or some non-specific binding (Buchwalow et al., 2011). Even if the phage itself had the capacity to bind to the tissue, it is clear that the modified phage has higher affinity than the wild type.

In the incubation of the modified phage with the AD model tissue, an intense staining can be observed covering the entire section. The staining could be observed all over the tissue, with more or less intensity in different brain areas. It is also important to notice that only the FITC filter shows fluorescence, without alterations in the images with DAPI filter. In opposition, the incubation of the modified phage with the healthy tissue showed no intensity at all, so no binding seemed to occur.

The APPswe/PS1dE9 model of AD is widely used in the study of Aβ plaques. Recent studies demonstrate a significant amyloid peptide deposition in the brain of these mice. With only 6 months old, it is clear the presence of Aβ oligomers (Pedrós, Petrov, Allgaier, Sureda, & Barroso, 2014). Reviewing the IHC results, we can state that the modified phage particle with the 4 amino acids of the recognition peptide (Aβ 36-39) has a high affinity to the AD model tissue.

Besides the high concentration of plaques in the tissue, another characteristic is its distribution. Resembling the distribution of Aβ plaques in the brains of humans, this AD model suggests the presence of Aβ plaques in olfactory structures, cerebral cortex, hippocampal formation, amygdala and cerebellum. Some exceptions were found in a few areas of the mouse model (Darvesh et al., 2012). The lack of Aβ plaques in areas of the brain suggests also a

decrease in the concentration of Aβ oligomers, which can explain the lower affinity of our phage particle in some brain zones.

These results were expected considering that, theoretically, a tissue with AD has higher concentrations of Aβ oligomers comparing to a tissue without the disease (Andreasen et al., 2013). This result supports the possibility of the Aβ sequence present in the phage capsid being specific for the Aβ oligomers. Although these results are very important to understand the disease, it is essential to note that AD mouse models are limited in their translation to human disease and only 1 % of AD cases in humans are linked to mutations. Additionally, even knowing that Aβ deposition is always present in AD, the chemical properties of these peptides can be different depending on how the disease was triggered (Wilhelmus et al., 2016).

The results of the modified phage were similar in several repetitions of the protocol. On the other hand incubation with the wild type phage showed variable staining. However, staining was always lower than the modified phage (see annex II for more photos). Therefore, even though very simple in concept, IHC protocols require care when executed. The fact that results are not always exactly the same is due to the existence of many variants that could affect the obtained results. The principal variants are: specimen treatment and fixation, tissue processing, antigen retrieval, antibody selection and the used IHC method (Matos et al., 2010; Unstan et al., 2011).

3.4.2 Double staining

The elaboration of this work is based on the assumption that the identified Aβ sequences only would be specific for the Aβ oligomers and fibrils. In order to reinforce the results obtained in single staining protocol further tests were carried out.

In this assay the same tissues were tested but in addition to the bacteriophages labeled with a FITC fluorochrome a second one, having high affinity to Aβ plaques, was also incubated. This incubation was expected to allow the identification of Aβ plaques, through a specific antibody labeled with a red fluorochrome. The Aβ oligomers and fibrils continued to be observed in the green channel.

Intracellular accumulation of Aβ peptide has been proposed as an early event in AD pathogenesis. So the identification of Aβ oligomers and amyloids plates is a crucial step to understand how AD biomarkers work (Panza et al., 2010). Many reports already demonstrate

how amyloid plaques are presented in the brain but few talk about the properties and dispersion of Aβ oligomers.

The single staining results have enabled us to assume that our particle had affinity to the Aβ oligomers. Through a double staining protocol it was possible to identify differences between the amyloid plaques and the Aβ oligomers (Figure 24).

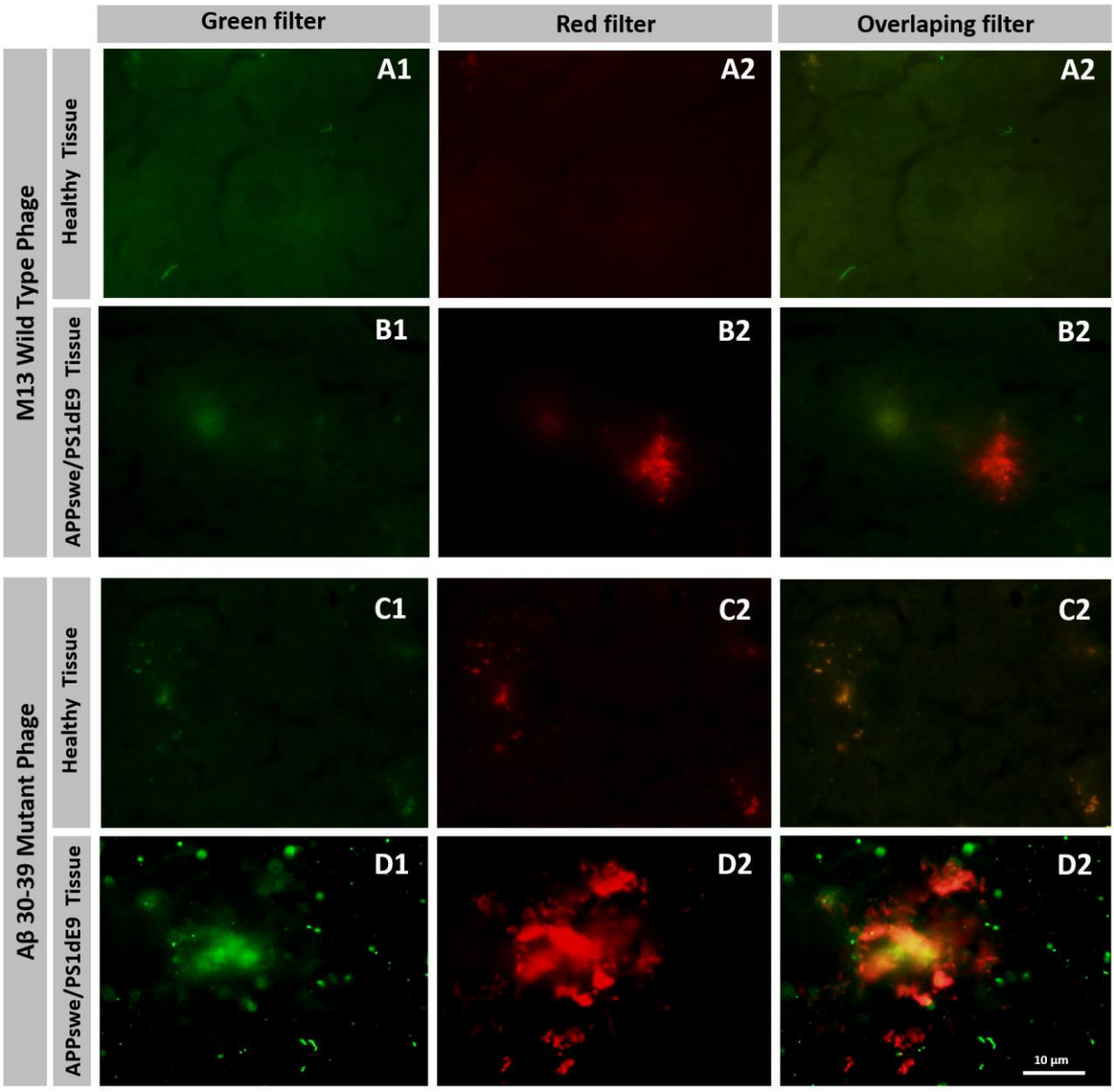

Figure 24 Epifluorescence images showing the M13 wild type and the Aβ 30-39 mutant phage particles incubated with samples of healthy tissue and AD model tissue. *Columns correspond to different microscope filters (FITC on the first column and TRITC on second). The third column represent the overlap of the two channels. A and B correspond to the M13 wild type incubation and C and D to the Aβ 30-39 mutant phage. All images were acquired using 100 × 1.30 NA oil objective lens.*

In the incubation of the M13 wild type phage, both tissues show no signs of staining when analyzed in FITC filter. These results support the data obtained from the single staining assays. Also it also was possible to observe amyloid plaques only in the AD model tissue. The incubation of the wild type phage serves as control in order to ensure that the staining is specific for the Aβ oligomers.

For the incubation of the modified phage with both tissues, an intense staining was observed in the FITC filter for the AD model tissue. In the healthy tissue no staining in FITC filter was observed. These results consolidate the results obtained in the single staining protocol. Additionally, an antibody labeled with a red fluorochrome with affinity to Aβ plaques was used. The APPswe/PS1dE9 transgenic mouse is known for the overproduction of Aβ peptide which leads to the deposit of Aβ plaques in some areas of the brain (Crouzin et al., 2013). As early as 6 month age this mouse model is already in the early onset human AD. At this stage the plaques are tiny but very compact what should allow clear visualization (Ruan et al., 2009).

The incubation of 6E10 antibody, allowed visualization of amyloids plaques in the AD model tissue. Despite the visualization of the plaques, its distribution was not homogeneous, with areas of visible plaques and others were no plaque could be observed. These results could sustain the different distribution of the Aβ peptides in the brain (Xiong et al., 2011). As expected, the presence of amyloid plaques was not observed in healthy tissue.

Despite very promising, the information given by these results is very limited. IHC tests can inform if two agents bind each other without providing the quantification of the affinity. In the future, it will be necessary to ensure that the modified phage is actually binding to the Aβ oligomers and not to contaminations in the tissue (Ferrier et al., 1999).

3.5 M13KE Chemical Functionalization

Although the chemical functionalization protocol of the M13KE phages (modified and wild type) had been started, it was not possible to obtain the functionalized phage particle

4. CONCLUSIONS

The main goal of this work was the development of an engineered phage particle for the early diagnosis of Alzheimer's disease.

The P3 coat protein from M13 phage was genetically modified in order to express on M13 surface the sequences described to have affinity to the Aβ oligomers and fibrils. Two sequences were used in this work, the Aβ 30-39 (AIIGLMVGGV) and Aβ 33-42 (LMVGGVVIA).

Throughout this work different approaches have been used to obtain a positive phage particle. In the first approach, two different ways for the design and formation of inserts were tested and in both the inserts of the two Aβ sequences were successfully obtained. During the many attempts and different protocol optimizations to clone each one of the Aβ sequences into the M13 genome, no positive clones were obtained.

A new approach was used - the Round PCR, designed to be able to insert a desired sequence into the phage DNA trough a PCR protocol. From this technique it was possible to obtain a particle phage containing the last four amino acids of the 10 amino acids of the sequence Aβ 30-39 (VGGV).

With this phage particle IHC assays were performed in order to assess the affinity of that sequence towards the Aβ oligomers/fibrils. When performing the IHC assays, two different tissues from the hippocampus region of 6 month-old mice were used: (i) slides of healthy mice and (ii) slides of double transgenic mice APPswe/PS1dE9 (an AD model characterized by the presence of Aβ oligomers and amyloid plaques). The results of these assays proved promising, showing a significant affinity of our modified phage towards the AD model tissue. Furthermore, the modified phage did not show affinity for the healthy tissue, and the wild type phage showed no affinity for any of the tissues.

To get more information about how our particle behaved in relation to the tissue, another incubation was carried out, however this time with the addition of an antibody specific for amyloid plaques. With this incubation it was possible to observe that the modified phage did not have an affinity for amyloid plaques and possibly only for the Aβ oligomers.

Regardless of the encouraging IHC results, in an attempt to create a phage particle with the whole Aβ sequence, one last approach was tried. The phagemid is a plasmid that can be used as a cloning vector in combination with filamentous phage M13. Using the phagemid, we

fused the DNA of a modified pETDuet-1 plasmid with the DNA of the M13KO7 helper phage. To the commercial pETDuet-1 plasmid some features were inserted, such as the P3 protein of M13 phage. Through a digestion/ligation protocol, the two Aβ sequences were successfully inserted into the plasmid DNA, right before the gene 3 zone. After cloning, the infection with the M13KO7 helper phage was performed and the phagemid particles were confirmed by sequencing. Regrettably, all samples proved to be negative.

From a general perspective, the general objectives of this work were achieved with relative success. Although the results prove promising, much work can be performed to improve the system. The discovery of a diagnostic tool for disorders such as AD is a very important milestone that will help many people in the future, and the use of bacteriophages may be the way to create an effective, inexpensive and well characterized instrument for early diagnosis.

5. FUTURE PERSPECTIVES

The application of phage as a tool for the diagnosis of Alzheimer's disease is a promising approach that must be considered in the future. Despite some of the main goals of this project had been achieved, much work remains to be done in order to validate the modification of M13 phage with the Aβ sequences.

For future studies, and in order to optimize the work performed during this project, the following experiments are suggested.

Use the petDuet-1 plasmid already containing the Aβ sequences to complete the formation of the phagemid particle. A positive phagemid will display the whole Aβ sequences. With the complete sequence is more likely to achieve a more specific affinity to Aβ oligomers.

Perform affinity ELISA assays using commercial Aβ oligomers and the mutant phage obtained in the Round PCR approach, which could indicate if our particle binds to the Aβ oligomers and also quantify the strength of this affinity.

Functionalize P8 protein of the modified phage with a fluorescent molecule in order to track and monitor this new particle in *in vivo* assay.

6. REFERENCES

Abbott, N. J., Patabendige, A. A. K., Dolman, D. E. M., Yusof, S. R., & Begley, D. J. (2010). Neurobiology of Disease Structure and function of the blood – brain barrier. *Neurobiology of Disease*, *37*(1), 13–25.

Abbott, N. J., Rönnbäck, L., & Hansson, E. (2006). Astrocyte – endothelial interactions at the blood – brain barrier. *Nano Reviews*, *7*(January), 41–53.

ADAM, A. C., GONZA´LEZ-BLASCO, G., RUBIO-TEXEIRA, M., & POLAINA, J. (1999). Transformation of Escherichia coli with DNA from Saccharomyces cerevisiae Cell Lysates. *Applied and Environmental Microbiology*, *65*(12), 5303–5306.

Alzheimer, A. (1907). Uber eine eigenartige Erkrankung der Hirnrinde. *Allg Zeits Psychi- Atry PsychischYGerichtlich Med*, *64*, 146–8.

Andreasen, N., Zetterberg, H., & Blennow, K. (2013). Evaluating Amyloid- b Oligomers in Cerebrospinal Fluid as a Biomarker for Alzheimer ' s Disease. *PLoS ONE*, *8*(6), 1–8.

Bäckman, L., Jones, S., Berger, a. K., Laukka, E. J., & Small, B. J. (2004). Multiple cognitive deficits during the transition to Alzheimer's disease. *Journal of Internal Medicine*, *256*, 195–204.

Bernard, J. M. L., & Francis, M. B. (2014). Chemical strategies for the covalent modification of filamentous phage. *Frontiers in Microbiology*, *5*(December), 1–7. 4

Brewer, G. J. (2012). Copper excess, zinc deficiency, and cognition loss in Alzheimer's disease. *BioFactors*, *38*, 107–113.

Buchwalow, I., Samoilova, V., Boecker, W., & Tiemann, M. (2011). Non-specific binding of antibodies in immunohistochemistry: fallacies and facts. *Scientific Reports*, *1*, 1–6.

Carol Turkington, Deborah R. M. (2010). *The Encyclopedia of Alzheimer's Disease* (2nd ed.).

Caselli, R. J., & Reiman, E. M. (2013). Characterizing the preclinical stages of Alzheimer's disease and the prospect of presymptomatic intervention. *Journal of Alzheimer's Disease : JAD*, *33 Suppl 1*, S405-16.

Chhibber, S., & Kumari, S. (2012). Application of Therapeutic Phages in Medicine. In *Immunology and Microbiology » "Bacteriophages"* (Ipek Kurtb, p. 256).

Chung, W.-J., Lee, D.-Y., & Yoo, S. Y. (2014). Chemical modulation of M13 bacteriophage and its functional opportunities for nanomedicine. *International Journal of Nanomedicine*, *9*, 5825–5836.

Crouzin, N., Baranger, K., Cavalier, M., Marchalant, Y., Cohen-Solal, C., Roman, F. S., Vignes, M. (2013). Area-specific alterations of synaptic plasticity in the 5XFAD mouse model of Alzheimer's disease: dissociation between somatosensory cortex and hippocampus. *PloS One*, *8*(9), e74667.

Darvesh, S., Cash, M. K., Reid, G. A., Martin, E., Mitnitski, A., & Geula, C. (2012). Butyrylcholinesterase is Associated with β-Amyloid Plaques in the Transgenic APP(SWE)/PSEN1dE9 Mouse Model of Alzheimer Disease. *Journal of Neuropathology and Experimental Neurology*, *71*(1), 2–14.

Dauwels, J., Vialatte, F.-B., & Cichocki, A. (2010). Diagnosis of alzheimers disease from eeg signals: Where are we standing? *Current Alzheimer Research*, *7*(Mci), 1–43.

DeMattos, R. B., Lu, J., Tang, Y., Racke, M. M., DeLong, C. a., Tzaferis, J. a., Hutton, M. L. (2012). A Plaque-Specific Antibody Clears Existing β-amyloid Plaques in Alzheimer's Disease Mice. *Neuron*, *76*(5), 908–920.

Donoso, A. (2003). Alzheimer disease. *Revista Chilena de Neuro-Psiquiatría*, *41*(2), 13–22.

Dor-On, E., & Solomon, B. (2015). Targeting glioblastoma via intranasal administration of Ff bacteriophages. *Frontiers in Microbiology*, *6*(MAY), 1–11.

Drulis-Kawa, Z., Majkowska-Skrobek, G., Maciejewska, B., Delattre, A.-S., & Lavigne, R. (2012). Learning from bacteriophages - advantages and limitations of phage and phage-encoded protein applications. *Current Protein & Peptide Science*, *13*(8), 699–722.

Dufouil, C., Clayton, D., Brayne, C., Chi, L. Y., Dening, T. R., Paykel, E. S., Huppert, F. A. (2000). Population norms for the MMSE in the very old: estimates based on longitudinal data. Mini-Mental State Examination. *Neurology*, *55*(11), 1609–1613.

Dunstan, R. W., Keith A., W. J., Quigley, C., & Lowe, A. (2011). The Use of Immunohistochemistry for Biomarker Assessment — Can It Compete with Other Technologies ? *Toxicologic Pathology*, *39*, 988–1002.

Eikelenboom, P., Van Exel, E., Hoozemans, J. J. M., Veerhuis, R., Rozemuller, A. J. M., & Van Gool, W. a. (2010). Neuroinflammation - An early event in both the history and pathogenesis of Alzheimer's disease. *Neurodegenerative Diseases*, *7*, 38–41.

Farr, R., Choi, D. S., & Lee, S. W. (2014). Phage-based nanomaterials for biomedical applications. *Acta Biomaterialia*, *10*(4), 1741–1750.

Ferrier, C. M., Witte, H. H. De, Straatman, H., Tienoven, D. H. Van, Geloof, W. L. Van, Rietveld, F. J. R., Ruiter, D. J. (1999). Comparison of immunohistochemistry with immunoassay (ELISA) for the detection of components of the plasminogen activation system in human tumour tissue, *British journal of cancer, 79*, 1534–1541.

Frenkel, D., & Solomon, B. (2002). Filamentous phage as vector-mediated antibody delivery to the brain. *Proceedings of the National Academy of Sciences of the United States of America*, *99*, 5675–5679.

Frenkel, D., Solomon, B., & Benhar, I. (2000). Modulation of Alzheimer ' s b-amyloid neurotoxicity by site-directed single- chain antibody, *Journal of Neuroimmunology, 106*, 23–31.

Fukunaga, K., & Taki, M. (2012). Practical tips for construction of custom Peptide libraries and affinity selection by using commercially available phage display cloning systems. *Journal of Nucleic Acids*, *2012*, 295719.

Gao, H. (2016). Progress and perspectives on targeting nanoparticles for brain drug delivery. *Acta Pharmaceutica Sinica B*, *6*(4), 268–286.

Georgieva, Y., & Konthur, Z. (2011). Design And Screening Of M13 phage display cDNA libraries. *Molecules*, 16, 1667-1681.

Georgieva, J. V, Brinkhuis, R. P., Stojanov, K., Weijers, C. A. G. M., Zuilhof, H., Rutjes, F. P. J. T., Zuhorn, I. S. (2012). Peptide-Mediated Blood – Brain Barrier Transport of Polymersomes ** Angewandte, 8339–8342.

Ghosh, D., Kohli, A. G., Moser, F., Endy, D., & Belcher, A. M. (2012). Refactored M13 bacteriophage as a platform for tumor cell imaging and drug delivery. *ACS Synthetic Biology*, *1*, 576–582.

Ghosh, D., Lee, Y., Thomas, S., Kohli, A. G., Yun, D. S., Belcher, A. M., & Kelly, K. A. (2012). M13-templated magnetic nanoparticles for targeted in vivo imaging of prostate cancer. *Nature Nanotechnology*, *7*(10), 677–682.

Haass, C., & Selkoe, D. J. (2007). Soluble protein oligomers in neurodegeneration: lessons from the Alzheimer's amyloid beta-peptide. *Nature Reviews. Molecular Cell Biology*, *8*(February), 101–112.

Hairul Bahara, N. H., Tye, G. J., Choong, Y. S., Ong, E. B. B., Ismail, A., & Lim, T. S. (2013). Phage display antibodies for diagnostic applications. *Biologicals*, *41*(4), 209–216.

Harper, D. (2011). Beneficial Use of Viruses. *Viruses: Biology, Applications, and Control*, 1–346.

Hashiguchi, S., Yamaguchi, Y., Takeuchi, O., Akira, S., & Sugimura, K. (2010). Biochemical and Biophysical Research Communications Immunological basis of M13 phage vaccine : Regulation under MyD88 and TLR9 signaling. *Biochemical and Biophysical Research Communications*, *402*(1), 19–22.

Hess, G. T., Cragnolini, J. J., Popp, M. W., Allen, M. A., Dougan, S. K., Spooner, E., Guimaraes, C. P. (2012). M13 bacteriophage display framework that allows sortase-mediated modification

of surface-accessible phage proteins. *Bioconjugate Chemistry*, *23*(7), 1478–1487.

Humpel, C. (2011). Identifying and validating biomarkers for Alzheimer's disease. *Trends in Biotechnology*, *29*(1), 26–32.

Iwatsubo, T., Odaka, A., Suzuki, N., Mizusawa, H., Nukina, N., & Ihara, Y. (1994). Visualization of A beta 42(43) and A beta 40 in senile plaques with end-specific A beta monoclonals: evidence that an initially deposited species is A beta 42(43). *Neuron*, *13*, 45–53.

Jack, C. R., Albert, M. S., Knopman, D. S., Mckhann, G. M., Sperling, R. A., Carrillo, M. C., Phelps, C. H. (2011). Introduction to the recommendations from the National Institute on Aging and the Alzheimer ' s Association workgroup on diagnostic guidelines for Alzheimer ' s disease. *Alzheimer's & Dementia*, *7*, 257–62.

Jankowsky, J. L., Xu, G., Fromholt, D., Gonzales, V., & Borchelt, D. R. (2003). Environmental enrichment exacerbates amyloid plaque formation in a transgenic mouse model of Alzheimer disease. *Journal of Neuropathology and Experimental Neurology*, *62*(12), 1220–1227.

Jin, H., Farr, R., & Lee, S. (2014). Biomaterials Collagen mimetic peptide engineered M13 bacteriophage for collagen targeting and imaging in cancer. *Biomaterials*, 35, 9236-9245.

Johnson, K. a., Minoshima, S., Bohnen, N. I., Donohoe, K. J., Foster, N. L., Herscovitch, P., Thies, W. H. (2013). Appropriate use criteria for amyloid PET: A report of the Amyloid Imaging Task Force, the Society of Nuclear Medicine and Molecular Imaging, and the Alzheimer's Association. *Alzheimer's and Dementia*, (January), 1–15.

Jones, A. R., Stutz, C. C., Zhou, Y., Marks, J. D., & Shusta, E. V. (2014). Identifying blood-brain-barrier selective single-chain antibody fragments. *Biotechnology Journal*, *9*, 664–674.

Kawasaki, T., Onodera, K., & Kamijo, S. (2011). Identification of Novel Short Peptide Inhibitors of Soluble 37/48 kDa Oligomers of Amyloid β42. *Bioscience, Biotechnology, and Biochemistry*, *75*(8), 1496–1501.

Kelly, K. a, Waterman, P., & Weissleder, R. (2006). In vivo imaging of molecularly targeted phage. *Neoplasia (New York, N.Y.)*, *8*(12), 1011–1018.

Kilby, B. A. (1976). Biochemistry, the molecular basis of cell structure and function: Albert L. Lehninger. Second Edition, 1975. Worth Publishers, Inc., New York. Pp. 1104. *Biochemical Education*, *4*(3), 61.

Kropinski, A. M. (2006). Phage therapy - Everything old is new again. *Canadian Journal of Infectious Diseases and Medical Microbiology*, *17*(5), 297–306.

Ksendzovsky, A., Walbridge, S., Saunders, R. C., Asthagiri, A. R., Heiss, J. D., & Lonser, R. R. (2012). Convection-enhanced delivery of M13 bacteriophage to the brain. *Journal of Neurosurgery*, 117, 197-203.

Kutter, E., De Vos, D., Gvasalia, G., Alavidze, Z., Gogokhia, L., Kuhl, S., & Abedon, S. T. (2010). Phage therapy in clinical practice: treatment of human infections. *Current Pharmaceutical Biotechnology*, *11*(1), 69–86.

LaFerla, F. M., Green, K. N., & Oddo, S. (2007). Intracellular amyloid-beta in Alzheimer's disease. *Nature Reviews. Neuroscience*, *8*(7), 499–509.

Larbanoix, L., Burtea, C., Ansciaux, E., Laurent, S., Mahieu, I., Vander Elst, L., & Muller, R. N. (2011). Design and evaluation of a 6-mer amyloid-beta protein derived phage display library for molecular targeting of amyloid plaques in Alzheimer's disease: Comparison with two cyclic heptapeptides derived from a randomized phage display library. *Peptides*, *32*(6), 1232–1243.

Leifer, B. P. (2003). Early Diagnosis of Alzheimer's Disease: Clinical and Economic Benefits. *Journal of the American Geriatrics Society*, *51*, 281–289.

Lesné, S. E., Sherman, M. a., Grant, M., Kuskowski, M., Schneider, J. a., Bennett, D. a., & Ashe, K. H. (2013). Brain amyloid-β oligomers in ageing and Alzheimer's disease. *Brain*, *136*, 1383–1398.

Li, J., Zhang, Q., & Pang, Z. (2012). Identification of peptide sequences that target to the brain using in vivo phage display. *Amino Acids*, *42*(6), 2373–2381. y

Li, J., Zhang, Q., Pang, Z., Wang, Y., Liu, Q., Guo, L., & Jiang, X. (2012). Identification of peptide sequences that target to the brain using in vivo phage display. *Amino Acids*, *42*(6), 2373–2381.

Li, K., Chen, Y., Li, S., Nguyen, H. G., Niu, Z., You, S., Wang, Q. (2010). Chemical modification of M13 bacteriophage and its application in cancer cell imaging. *Bioconjugate Chemistry*, *21*(7), 1369–1377.

Lim, A., & Lim, A. (2013). Alzheimer ' s Disease : A Historical Perspective. *Sound Neuroscience: An Undergraduate Neuroscience Journal*, *1*(1), 7–10.

Liu, H., & Naismith, J. H. (2008). An efficient one-step site-directed deletion, insertion, single and multiple-site plasmid mutagenesis protocol. *BMC Biotechnology*, *10*, 1–10.

Loc-Carrillo, C., & Abedon, S. T. (2011). Pros and cons of phage therapy. *Bacteriophage*, *1*(2), 111–114.

Lund, P. E., Hunt, R. C., Gottesman, M. M., & Kimchi-Sarfaty, C. (2010). Pseudovirions as vehicles for the delivery of siRNA. *Pharmaceutical Research*, *27*(3), 400–420.

MacLeod, R., Hillert, E.-K., Cameron, R. T., & Baillie, G. S. (2015). The role and therapeutic targeting of α - , β - and γ -secretase in Alzheimer ' s disease. *Future Science OA*, *1*(3).

Matos, L. L. de, Trufelli, D. C., Matos, M. G. L. de, & Pinhal, M. A. da S. (2010). Immunohistochemistry as an Important Tool in Biomarkers Detection and Clinical Practice.

Biomarker Insights, *5*(1841), 9–20.

Matsuda, H. (2007). Role of neuroimaging in Alzheimer's disease, with emphasis on brain perfusion SPECT. *Journal of Nuclear Medicine : Official Publication, Society of Nuclear Medicine*, *48*(8), 1289–1300.

Matsunaga, S., Kishi, T., & Iwata, N. (2015). Memantine monotherapy for Alzheimer's Disease:A systematic review and meta-analysis. *PLoS ONE*, *10*(4), 1–16.

Maurer, K., Volk, S., & Gerbaldo, H. (1997). Auguste D and Alzheimer ' s disease. *The Lancet*, *349*(9064), 1906–1909.

McKhann, G. M., Knopman, D. S., Chertkow, H., Hyman, B. T., Jack, C. R., Kawas, C. H., Phelps, C. H. (2011). The diagnosis of dementia due to Alzheimer's disease: Recommendations from the National Institute on Aging-Alzheimer's Association workgroups on diagnostic guidelines for Alzheimer's disease. *Alzheimer's and Dementia*, *7*(3), 263–269.

Meek, P. D., McKeithan, E. K., & Schumock, G. T. (1998). Economic Considerations in Alzheimer's Disease. *Pharmacotherapy: The Journal of Human Pharmacology and Drug Therapy*, *18*, 68–73.

Miller, Y., Ma, B., & Nussinov, R. (2010). Zinc ions promote Alzheimer Abeta aggregation via population shift of polymorphic states. *Proceedings of the National Academy of Sciences of the United States of America*, *107*(21), 9490–9495.

Moon, J.-S., Kim, W.-G., Kim, C., Park, G.-T., Heo, J., Yoo, S. Y., & Oh, J.-W. (2015). M13 Bacteriophage-Based Self-Assembly Structures and Their Functional Capabilities. *Mini-Reviews in Organic Chemistry*, *12*(3), 271–281.

Nazem, A., & Mansoori, G. A. (2008). Nanotechnology solutions for Alzheimer's disease: advances in research tools, diagnostic methods and therapeutic agents. *Journal of Alzheimer's Disease : JAD*, *13*(2), 199–223.

Ngweniform, P., Abbineni, G., Cao, B., & Mao, C. (2009). Self-assembly of drug-loaded liposomes on genetically engineered target-recognizing M13 phage: A novel nanocarrier for targeted drug delivery. *Small*, *5*(17), 1963–1969.

Nordberg, A. (2015). The use of amyloid imaging in clinical praxis : a critical review. *Clinical and Translational Imaging*, *3*(1), 7–11.

Noren, K. A., & Noren, C. J. (2001). Construction of High-Complexity Combinatorial Phage Display Peptide Libraries. *Methods*, *178*, 169–178.

Nowotny, P., M Kwon, J., & M Goate, A. (2001). Alzheimer Disease. *Encyclopedia of Life Sciences*, 1–6.

Ohtsuki, S., & Terasaki, T. (2007). Contribution of carrier-mediated transport systems to the blood-

brain barrier as a supporting and protecting interface for the brain; importance for CNS drug discovery and development. *Pharmaceutical Research*, 24, 1745-1758.

Panza, F., Frisardi, V., Imbimbo, B. P., Capurso, C., Logroscino, G., Sancarlo, D., Solfrizzi, V. (2010). γ -Secretase Inhibitors for the Treatment of Alzheimer ' s Disease : The Current State. *CNS Neuroscience & Therapeutics*, *16*, 272–284.

Parsons, C. G., Danysz, W., Dekundy, A., & Pulte, I. (2013). Memantine and cholinesterase inhibitors: Complementary mechanisms in the treatment of Alzheimer's disease. *Neurotoxicity Research*, *24*(3), 358–369.

Paula, V. D. J. R. De, & Guimarães, F. M. (2009). Neurobiological pathways to Alzheimer's disease Amyloid-beta , Tau protein or both ? *Dementia & Neuropsychologia*, *3*(3), 188–194.

Pedrós, I., Petrov, D., Allgaier, M., Sureda, F., & Barroso, E. (2014). Biochimica et Biophysica Acta Early alterations in energy metabolism in the hippocampus of APPswe / PS1dE9 mouse model of Alzheimer ' s disease. *BBA - Molecular Basis of Disease*, *1842*(9), 1556–1566.

Perchiacca, J. M., Ladiwala, a. R. a., Bhattacharya, M., & Tessier, P. M. (2012). Structure-based design of conformation- and sequence-specific antibodies against amyloid . *Proceedings of the National Academy of Sciences*, *109*(1), 84–89.

Phipps, M. L., Lillo, A. M., Shou, Y., Schmidt, E. N., Paavola, C. D., Naranjo, L., Martinez, J. S. (2016). Beyond Helper Phage: Using "Helper Cells" to Select Peptide Affinity Ligands. *Plos One*, *11*(9), e0160940.

Pointer, K. B., Clark, P. A., Zorniak, M., Alrfaei, B. M., & Kuo, J. S. (2014). Glioblastoma cancer stem cells: Biomarker and therapeutic advances. *Neurochemistry International*, *71*(1), 1–7.

Pranjol, Z. I., & Hajitou, A. (2015). Bacteriophage-Derived Vectors for Targeted Cancer Gene Therapy. *Viruses*, *7*, 268–284.

Prince, M., Karagiannidou, M., Comas-Herrera, A., Knapp, M., & Guerchet, M. (2016). World Alzheimer Report 2016 Improving healthcare for people living with dementia. *Alzheimer's Disease International*.

Prisco, A., & de Berardinis, P. (2012). Filamentous bacteriophage Fd as an antigen delivery system in vaccination. *International Journal of Molecular Sciences*, *13*(4), 5179–5194.

Puzzo, D., Lee, L., Palmeri, A., Calabrese, G., & Arancio, O. (2014). Behavioral assays with mouse models of Alzheimer's disease: practical considerations and guidelines. *Biochemical Pharmacology*, *88*(4), 450–467.

Qi, H., Lu, H., Qiu, H., Petrenko, V., & Liu, A. (2012). Phagemid Vectors for Phage Display : Properties , Characteristics and Construction. *Journal of Molecular Biology*, *417*(3), 129–143.

Rajaram, K., & Vermeeren, V. (2014). Construction of helper plasmid-mediated dual-display phage

for autoantibody screening in serum. *Applied Microbiology and Biotechnology*, *98*, 6365–6373.

Rakonjac, J., Bennett, N. J., Spagnuolo, J., Gagic, D., & Russel, M. (2011). Filamentous bacteriophage: biology, phage display and nanotechnology applications. *Current Issues in Molecular Biology*, *13*(2), 51–76.

Rakover, I. S., Zabavnik, N., Kopel, R., Paz-Rozner, M., & Solomon, B. (2010). Antigen-specific therapy of EAE via intranasal delivery of filamentous phage displaying a myelin immunodominant epitope. *Journal of Neuroimmunology*, *225*(1–2), 68–76.

Rangel, R., Dobroff, A. S., Guzman-Rojas, L., Salmeron, C. C., Gelovani, J. G., Sidman, R. L., Arap, W. (2013). Targeting mammalian organelles with internalizing phage (iPhage) libraries. *Nature Protocols*, *8*(10), 1916–1939.

Richards, D., & Sabbagh, M. N. (2014). Florbetaben for PET Imaging of Beta-Amyloid Plaques in the Brain. *Neurology and Therapy*, *3*, 79–88.

Rooy, I. Van, Cakir-tascioglu, S., Couraud, P., Romero, I. A., Weksler, B., Storm, G., Mastrobattista, E. (2010). Identification of Peptide Ligands for Targeting to the Blood-Brain Barrier. *Pharmaceutical Research*, *27*(4).

Ruan, L., Kang, Z., Pei, G., & Le, Y. (2009). Amyloid Deposition and Inflammation in APPswe / PS1dE9 Mouse Model of Alzheimers Disease Amyloid Deposition and Inflammation in APPswe / PS1dE9 Mouse Model of Alzheimer ' s Disease. *Current Alzheimer Research*, *6*, 531–540.

Rudolph, S., Klein, A. N., Tusche, M., Schlosser, C., Elfgen, A., Brener, O., Willbold, D. (2016). Competitive Mirror Image Phage Display Derived Peptide Modulates Amyloid Beta Aggregation and Toxicity. *PLoS ONE*, *11*(2), 1–22.

Schmidt, R., Schmidt, H., Curb, J. D., Masaki, K., White, L. R., & Launer, L. J. (2002). Early inflammation and dementia: A 25-year follow-up of the Honolulu-Asia Aging Study. *Annals of Neurology*, *52*, 168–174.

Schmiedl, A., Breitling, F., Winter, C. H., Queitsch, I., & Dubel, S. (2000). Effects of unpaired cysteines on yield, solubility and activity of different recombinant antibody constructs expressed in E. coli. *Journal of Immunological Methods*, *242*(1–2), 101–114.

Schneider, L. S. (2013). Alzheimer Disease Pharmacologic Treatment and Treatment Research. *Continuum*, *19*, 339–357.

Schu, M. C., Sherva, R., Farrer, L. a, & Green, R. C. (2012). The Genetics of Alzheimer ' s sonal. *Alzheimer's Disease – Modernizing Concept, Biological Diagnosis and Therapy*, *28*, 15–29.

Seow, Y., Yin, H., & Wood, M. J. A. (2010). Peptides Identification of a novel muscle targeting

peptide in mdx mice. *Peptides*, *31*(10), 1873–1877.

Sevigny, J., Chiao, P., Bussière, T., Weinreb, P. H., Williams, L., Maier, M., Rhodes, K. (2016). The antibody aducanumab reduces A β plaques in Alzheimer ' s disease. *Nature Publishing Group*, *537*(7618), 50–56.

Shanmugam, A., Monien, B., & Bitan, G. (2008). Development in Diagnostic and Therapeutic Strategies for Alzheimer's Disease. In M.-K. S. Sun (Ed.), *Research Progress in Alzheimer's Disease and Dementia* (pp. 193–250).

Sheng, M., Sabatini, B. L., & Su, T. C. (2015). Synapses and Alzheimer ' s Disease. *Cold Spring Harbor Perspectives in Biology*, *4*, a005777.

Smith, G. P. (1985). Filamentous fusion phage: novel expression vectors that display cloned antigens on the virion surface. *Science (New York, N.Y.)*, *228*(4705), 1315–1317.

Smith, M. W., Al-jayyoussi, G., & Gumbleton, M. (2012). Peptides Peptide sequences mediating tropism to intact blood – brain barrier : An in vivo biodistribution study using phage display. *Peptides*, *38*(1), 172–180.

Solomon, B. (2008). Filamentous bacteriophage as a novel therapeutic tool for Alzheimer's disease treatment. *Journal of Alzheimer's Disease : JAD*, *15*(2), 193–198.

Tiraboschi, P., Hansen, L. a, Thal, L. J., & Corey-Bloom, J. (2004). The importance of neuritic plaques and tangles to the development and evolution of AD. *Neurology*, *62*(9127), 1984–1989.

Vaks, L., & Benhar, I. (2011). In vivo characteristics of targeted drug-carrying filamentous bacteriophage nanomedicines. *Journal of Nanobiotechnology*, *9*, 1–10.

Van Groen, T., Kadish, I., Funke, S. A., Bartnik, D., & Willbold, D. (2013). Treatment with D3 removes amyloid deposits, reduces inflammation, and improves cognition in aged AβPP/PS1 double transgenic mice. *Journal of Alzheimer's Disease*, *34*(3), 609–620.

Vargas-Sanchez, K., Vekris, A., & Petry, K. G. (2016). DNA Subtraction of In Vivo Selected Phage Repertoires for Efficient Peptide Pathology Biomarker Identification in Neuroinflammation Multiple Sclerosis Model. *Libertas Academica*, *11*, 19–29.

Waldemar, G., Dubois, B., Emre, M., Georges, J., McKeith, I. G., Rossor, M., Winblad, B. (2007). Recommendations for the diagnosis and management of Alzheimer's disease and other disorders associated with dementia: EFNS guideline. *European Journal of Neurology*, *14*, 1–26.

Wilfinger, W. W., Mackey, K., & Chomczynski, P. (1997). *Effect of pH and ionic strength on the spectrophotometric assessment of nucleic acid purity.* (Technical Report). *BioTechniques* (Vol. 22). England.

Wilhelmus, M. M. M., Jager, M. de, Smit, A. B., Loo, R. J. van der, & Drukarch, B. (2016). Catalytically active tissue transglutaminase colocalises with A β pathology in Alzheimer ' s disease mouse models. *Scientific Reports*, *6*(October 2015), 1–12.

Wu, W.-L., & Zhang, L. (2009). g-Secretase Inhibitors for the Treatment of Alzheimer's Disease. *Drug Development Research*, *70*, 94–100.

Xiong, H., Callaghan, D., Wodzinska, J., Xu, J., Premyslova, M., Liu, Q., & Con-, J. (2011). Biochemical and behavioral characterization of the double transgenic mouse model (APPswe / PS1dE9) of Alzheimer ' s disease. *Neuroscience Bulletin*, *27*(4), 221–232.

Zhang, Y., & Pardridge, W. M. (2001). Rapid transferrin efflux from brain to blood across the blood-brain barrier. *Journal of Neurochemistry*, *76*(5), 1597–1600.

Zhou, B., Dong, Q., Ma, R., Chen, Y., Yang, J., Sun, L.-Z., & Huang, C. (2009). Rapid isolation of highly pure single-stranded DNA from phagemids. *Analytical Biochemistry*, *389*(2), 177–179.

ANNEX I – ELECTROPHORESIS GELS

Results for Aβ 30-39 insert cloning in pETDuet-1 plasmid.

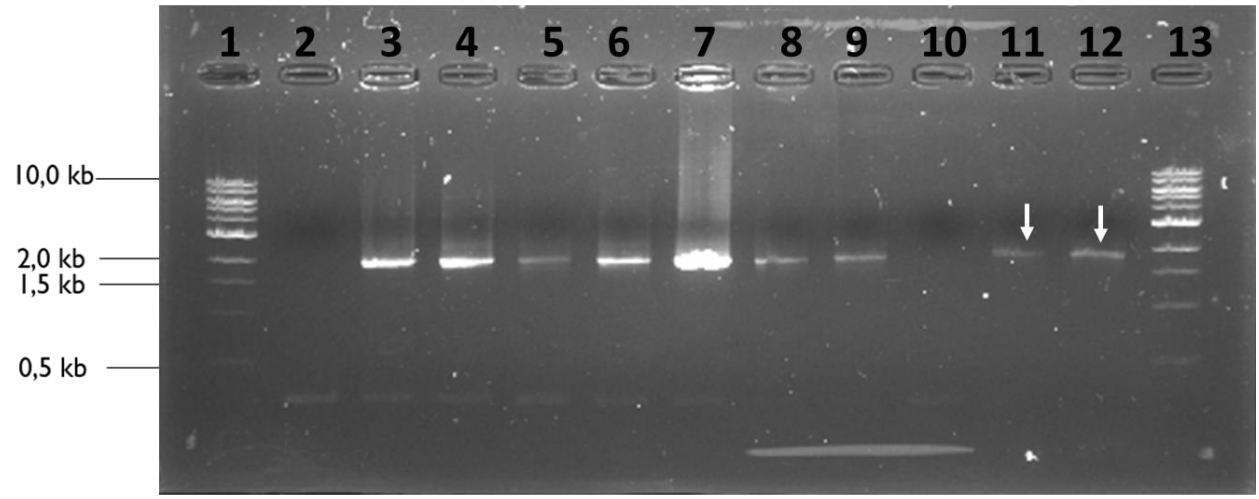

Figure 25 Gel electrophoresis results of an amplification of the gene 3 zone from pETDuet-1, containing the Aβ 30-39 sequence. Samples were loaded on 1 % agarose gel. *1 and 13 – 1 kb DNA ladder; 2-6 - Aβ 30-39 clones (1-5); 7- negative control (plasmid without insert); 8-12 - Aβ 30-39 Clones (6-10) ; Red arrows show the clones with different sizes comparing to the negative control band.*

ANNEX II – IMMUNOHISTOCHEMISTRY FIGURES

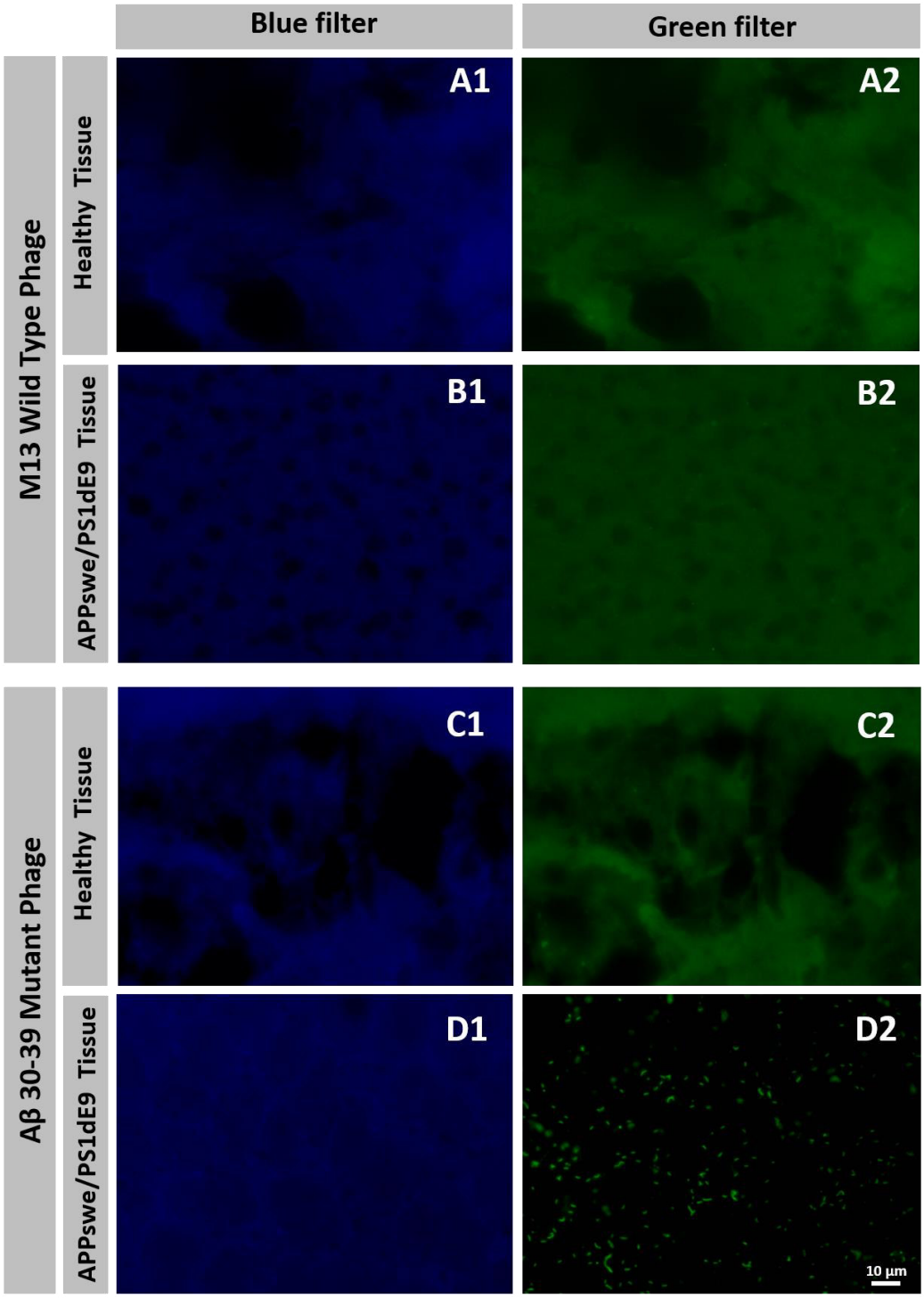

Figure 26 Epifluorescence images showing the M13 wild type and the Aβ 30-39 mutant phage particles incubated with samples of healthy tissue and AD model tissue. *Columns correspond to different microscope filters (DAPI on the left and FITC on the right) and lines A and B correspond to the M13 wild type incubation and C and D to the Aβ 30-39 mutant phage. All images were acquired using 100 × 1.30 NA oil objective lens.*

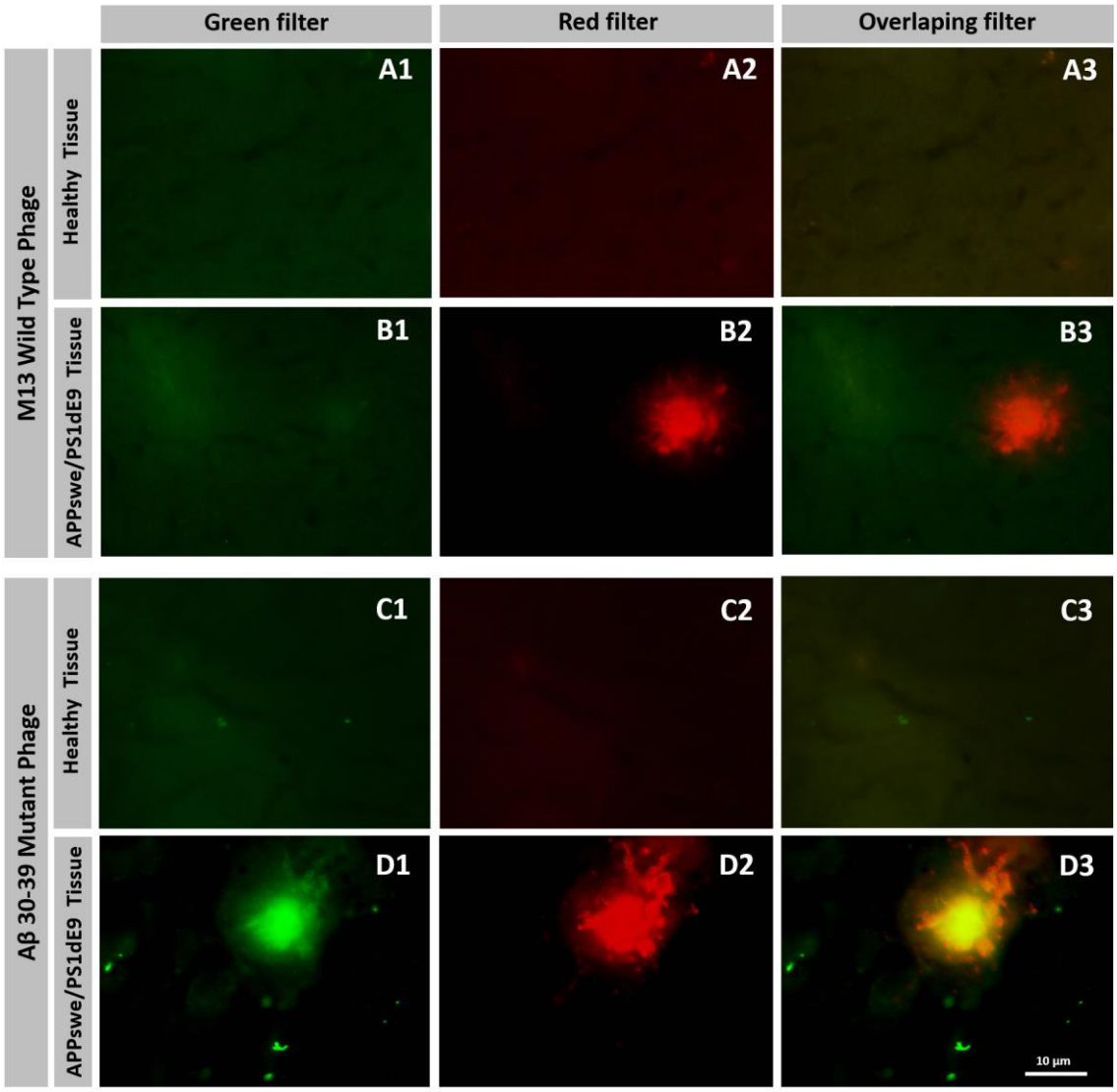

Figure 27 Epifluorescence images showing the M13 wild type and the Aβ 30-39 mutant phage particles incubated with samples of healthy tissue and AD model tissue. *Columns correspond to different microscope filters (FITC on the first column and TRITC on second). The third column represent the overlap of the two channels. Lines A and B correspond to the M13 wild type incubation and C and D to the Aβ 30-39 mutant phage. All images were acquired using 100 × 1.30 NA oil objective lens.*